

and incubated in primary antibody solution in blocking buffer for 30 minutes at 37°C and fluorescence labeling was performed with secondary antibodies, followed by propidium iodide for 5 minutes at room temperature to counterstain nuclei. The stained samples were observed under an Olympus Fluoview confocal laser-scanning microscope (Olympus).

Electron Microscopy

Neonatal skin samples and skin grafts were fixed in 5% glutaraldehyde solution, post fixed in 1% OsO₄, dehydrated, and embedded in Epon 812 (TAAB Laboratories, Berkshire, UK). All of the samples were ultra-thin sectioned at a thickness of 70 nm, and stained with uranyl acetate and lead citrate. Photographs were taken using a Hitachi H-7100 transmission electron microscope (Hitachi, Tokyo, Japan).

Lipid Analysis

Lipid analysis was performed as previously reported.⁹ Briefly, lipid analysis was done independently on three *Abca12*^{-/-} neonates, two wild-type as controls, and two mature *Abca12*^{-/-} skins 3 months after skin grafting and two mature wild-type skins 3 months after transplantation as control. We separated the epidermis from whole skin specimens of control and *Abca12*^{-/-} mice by incubation in sterile water at 60°C for 1 minute and homogenized in 0.8 ml of PBS. A total lipid component was extracted from tissue homogenates of epidermis according to conventional methods.⁹ Lipid analysis in epidermal lysates from neonates and grafted skin was performed by liquid chromatography, electrospray ionization mass spectrometry (LC-ESI-MS) using a HP 1100 liquid chromatography system (Agilent Technologies, Palo Alto, CA).

Measurement of Transepidermal Water Loss

Transepidermal water loss (TEWL) from the skin of neonatal mice and from skin grafted onto SCID mice was measured by evaporimeter (AS-VT100RS; AsahiBiomed Corp., Yokohama, Japan), as described previously.⁵ The AS-VT100RS utilizes the ventilated-chamber method for measuring TEWL. Its hygrometer measures the humidity of incoming air and of outgoing air that has passed over the test area of the skin, and TEWL is calculated from the difference. TEWL measurements were performed on the back of the neonates and the grafted skin onto the back of SCID mice.

Complementary DNA Microarray Analysis for the Gene Expression Profile

Total RNA isolated from primary/subcultured *Abca12*^{-/-} keratinocytes was extracted as described above. Total RNA concentration was calculated spectrophotometrically, and quality control of RNA was analyzed with an Agilent 2100 Bioanalyzer (Agilent Technologies, Tokyo, Japan). mRNA/cDNA hybrids were generated via T7oligo dT primers, fol-

lowed by addition of DNA polymerase and ligase (Filgen, Nagoya, Japan) to obtain double-stranded cDNA. The sample tagged with chemiluminescent substrate, Cy3 for the subcultured *Abca12*^{-/-} keratinocytes, or Cy5 for the primary-cultured *Abca12*^{-/-} keratinocytes, was hybridized on a microarray chip (Filgen Array mouse 32K, Filgen). We used a mixture of total RNAs from the two cultures for labeling reactions. Fluorescence images for Cy3 and Cy5 dye channels were obtained using a GenePix 4000B scanner (Axon Instruments, CA) and scan data images were analyzed using Microarray Data Analysis Tool version 3.0 software (Filgen).

Therapeutic Trial with Retinoids on Primary-Cultured Abca12^{-/-} Keratinocytes and Grafted Harlequin Ichthyosis Model Mice Skin

To test the efficacy of a therapeutic trial on primary-cultured *Abca12*^{-/-} keratinocytes, isotretinoin (purchased by Sigma Chemical Co., St. Louis, MO) was dissolved in dimethyl sulfoxide (DMSO). In addition, etretinate powder (a gift from Chugai Pharmaceuticals, Tokyo, Japan) was dissolved in sterile water.

Primary-cultured keratinocytes were grown in CnT-57 medium (CellIntec Advanced Cell Systems) and then switched into CnT-02 medium (CellIntec Advanced Cell Systems). Twenty-four hours later, the calcium concentration was changed to 1.2 mmol/L in CnT-02 medium with retinoids (10⁻⁶mol/L isotretinoin or 10⁻⁶mol/L etretinate) dissolved in DMSO or water. The final concentration of DMSO in medium was 0.01%. As control, keratinocytes were cultured in CnT-02 medium with 1.2 mmol/L calcium supplemented with 0.01% DMSO without retinoids. Forty-eight hours later, we extracted protein from keratinocytes.

In a therapeutic trial using grafted HI model mice skin, we dissolved several doses of isotretinoin in soy oil, and single doses (1, 10 mg/kg) of isotretinoin were administered orally into the grafted SCID mice 3 weeks after skin transplantation every day for 10 days.

Statistical Analysis

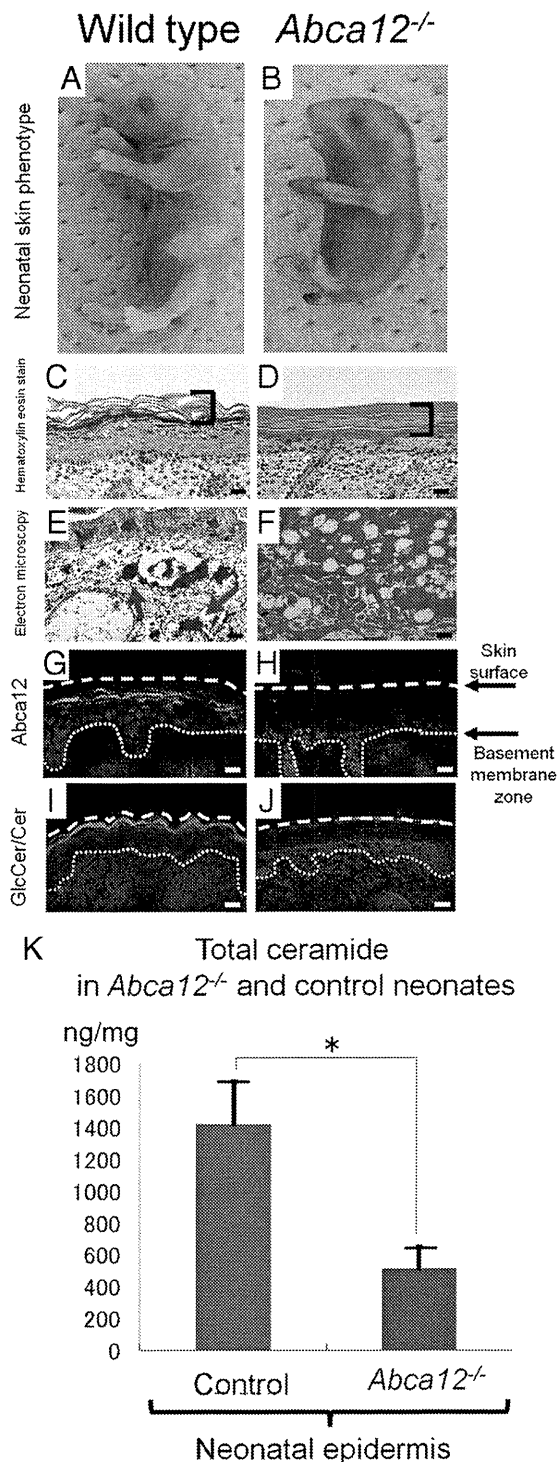
All statistical analyses were performed using student's *t*-tests with sample sizes indicated in the figure legends for each comparison that was made. *P* values of <0.05 were considered statistically significant.

Results

Abca12^{-/-} Neonatal Mouse Epidermis Exhibited Defective Lipid Distribution, Reduced Expression of Differentiation-Specific Proteins and Profilaggrin/Filaggrin Conversion Defects

As we previously reported,⁵ *Abca12*^{-/-} mice (Figure 1B) were typically born with a smaller body size than that of wild-type mice (Figure 1A). Erythematous, rigid skin covered the entire body surface of *Abca12*^{-/-} neonates.

Light microscopy showed a thick, compact cornified layers without the normal basket-weave appearance in the *Abca12*^{-/-} neonatal skin (Figure 1D), compared with normal neonatal skin (Figure 1C). Electron microscopy of *Abca12*^{-/-} neonatal skin showed numerous lipid droplets in the granular layer cell cytoplasm (Figure 1F). In wild-type neonatal skin, no lipid droplets were seen although normal keratohyalin granules were observed (Figure 1E). Immunofluorescence staining (Figure 1, G and H)



showed *Abca12* in wild-type but not *abca12*^{-/-} mice, with the glucosylceramide/ceramide distribution remarkably sparse at the *Abca12*^{-/-} neonatal mice granular/cornified layer interface (Figure 1J), compared with the intense labeling in the wild-type neonatal epidermis (Figure 1I). To verify these results in the neonatal *Abca12*^{-/-} and wild-type skin, we performed lipid analysis using skin samples from both the *Abca12*^{-/-} and wild-type neonates. Total amounts of epidermal ceramides were significantly reduced in *Abca12*^{-/-} neonatal mice (Figure 1K). Particularly, amounts/compositions of the CER[EOS], ceramide classes consisting of ester-linked non-hydroxy fatty acids, ω -hydroxy fatty acids and 4-sphinginenines, in *Abca12*^{-/-} neonatal epidermis were extremely small compared with control mice (see Supplemental Figure S1, A and B at <http://ajp.amjpathol.org>).

Immunofluorescence staining revealed that the keratinocyte differentiation (keratinization)-specific molecules, kallikrein 5 (KLK5), transglutaminase 1 (TGase1), and loricrin, were sparsely distributed in the upper epidermis of neonatal *Abca12*^{-/-} mice (Figure 2A–J). Immunofluorescence staining for KLK5, a lamellar granule component, was weak in *Abca12*^{-/-} neonatal mice granular layer (Figure 2B), in contrast to intense labeling in granular and lower cornified layers of wild-type neonatal skin (Figure 2A). *In situ* TGase1 activity assays with dansylcadaverine as a substrate showed neonatal *Abca12*^{-/-} granular layer keratinocytes exhibited weak TGase1 activity restricted to the cytoplasm (Figure 2D), compared with distinct TGase1 activity with a more peripheral pattern throughout neonatal wild-type granular layer keratinocytes (Figure 2C). Immunofluorescence staining showed loricrin expressed sparsely within neonatal *Abca12*^{-/-} granular layer cells (Figure 2F), compared with more intense expression in neonatal wild-type granular layer keratinocytes (Figure 2E).

KLK5, involucrin, TGase1, loricrin, and filaggrin mRNA expression was up-regulated in neonatal *Abca12*^{-/-} epidermal keratinocytes (Figure 2K). In contrast, protein expression using epidermal extract, Western blotting demonstrated that loricrin and KLK5 protein expression was reduced in neonatal *Abca12*^{-/-} epidermal keratinocytes compared with that in neonatal wild-type epidermis (Figure 2L). There were no significant differences in the pro-

Figure 1. *Abca12*^{-/-} neonatal phenotype and lipid trafficking defects. **A** and **B:** Gross phenotypes of wild-type and *Abca12*^{-/-} neonates. **C** and **D:** Light microscopy showed a thick compact cornified layer (bracket) without the normal basket-weave appearance in the *Abca12*^{-/-} mouse skin (**D**), compared with normal neonatal skin (**C**) (H&E stain; original magnification, $\times 40$) (Scale bars = 20 μ m). **E** and **F:** An electron micrograph of the *Abca12*^{-/-} neonatal skin showed numerous lipid droplets in the cytoplasm of the granular layer cells (**F**, red arrows). In the wild-type neonatal skin, no lipid droplets were seen and normal keratohyalin granules were observed (**E**, red arrows) (original magnification, $\times 3000$) (Scale bars = 2 μ m). **G** and **H:** By immunofluorescence staining, *Abca12* expression (Alexa488, green) was detected in the wild-type neonatal mouse skin (**G**), but not in the *Abca12*^{-/-} skin (**H**). **I** and **J:** Immunofluorescence staining showed the glucosylceramide/ceramide (GlcCer/Cer) (Alexa 488, green), a major lipid component of lamellar granules and an essential component of the epidermal permeability barrier, to be distributed remarkably sparse in the *Abca12*^{-/-} neonatal mouse granular/cornified layer interface (**J**), compared with the intense labeling in the wild-type neonatal epidermis (**I**). **K:** In neonatal mice, total ceramides levels were significantly reduced in the epidermis of *Abca12*^{-/-} mice. (*Abca12*^{-/-} neonates, *n* = 3; control neonates, *n* = 2) (**P* < 0.01). GlcCer, glucosylceramide; Cer, ceramide.

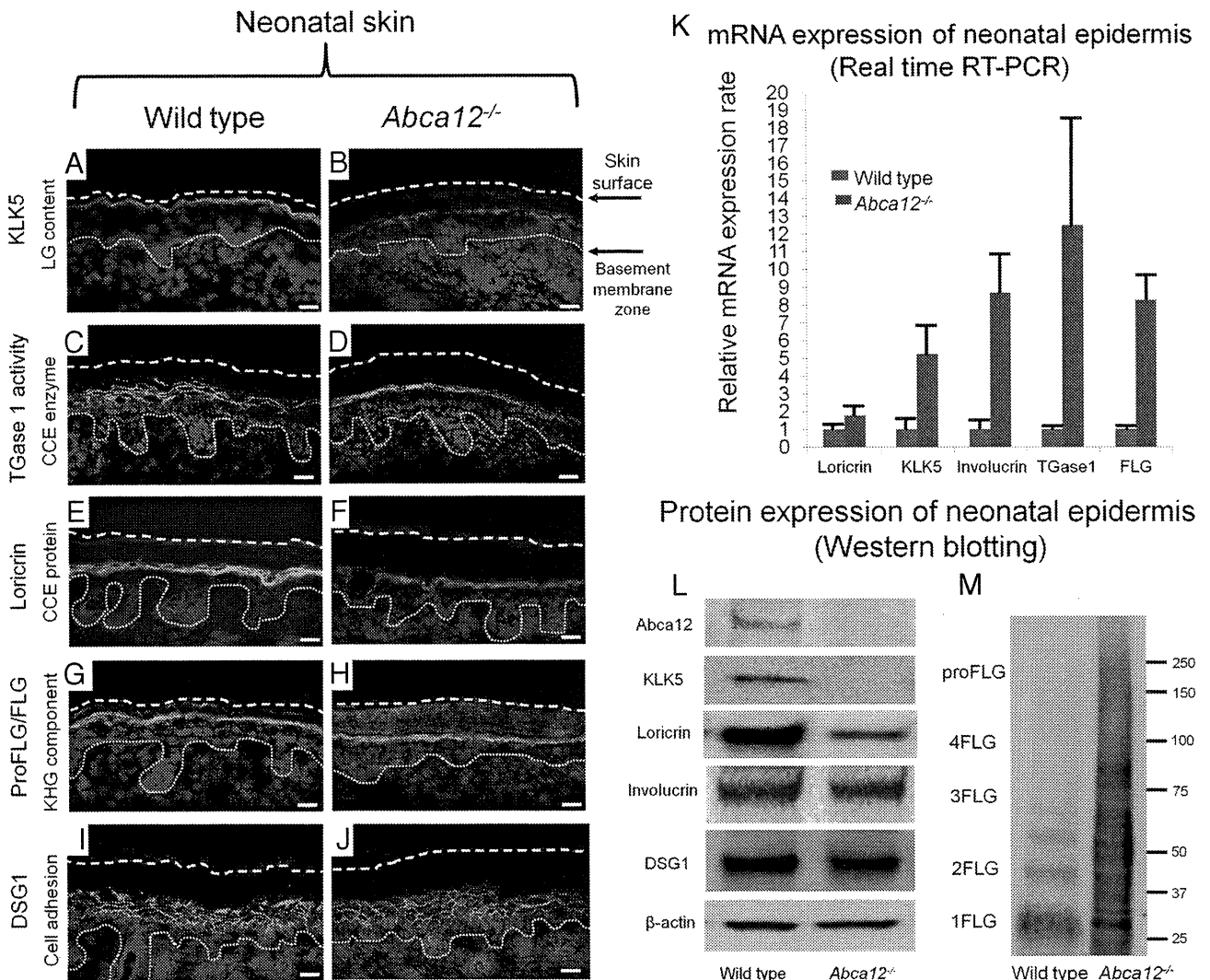


Figure 2. Reduced epidermal differentiation-associated molecules and defective conversion of profilaggrin to filaggrin in *Abca12*^{-/-} neonates. **A and B:** Immunofluorescence staining for kallikrein 5 (KLK5) (Alexa488, green), one of the lamellar granule (LG) contents, was weak in the *Abca12*^{-/-} neonatal mice granular keratinocyte layers (**B**), in contrast to its intense labeling in the granular layers and lower cornified layers of wild-type neonatal skin (**A**). **C and D:** *In situ* transglutaminase 1 (TGase1) activity assay (fluorescein isothiocyanate, green) with dansyl-cadaverine showed the granular layer keratinocytes in the *Abca12*^{-/-} neonates had weak transglutaminase 1 activity only in the cytoplasm (**D**), compared with distinct transglutaminase 1 activity with the peripheral pattern throughout granular layer keratinocytes in the wild-type neonates (**C**). Cytoplasmic localization of transglutaminase 1 in *Abca12*^{-/-} neonates indicated its inability to bind to the cell membrane and to therefore function at its proper place despite the significantly enhanced mRNA expression of transglutaminase 1 (see Figure 2K). **E and F:** Immunofluorescence staining showed loricrin (Alexa 488, green) expressed sparsely in the *Abca12*^{-/-} neonatal mice granular layer (**F**), compared with its intense expression in the granular layer of the wild-type neonatal skin (**E**). **G and H:** Both *Abca12*^{-/-} and wild-type neonatal skin showed intense profilaggrin/filaggrin (proFLG/FLG) (Alexa488, green) expression in the granular layer keratinocytes. However, in *Abca12*^{-/-} neonatal skin, profilaggrin/filaggrin distribution was also observed throughout the cornified layers. **I and J:** Desmoglein 1 (DSG1) (Alexa 488, green), a cell adhesion molecule unassociated with keratinization, was expressed at the cell periphery in the lower granular and spinous layers of the both *Abca12*^{-/-} neonatal skin and wild-type mouse skin. (nuclear stain; propidium iodide, red, **dotted lines**, the skin surface). Original magnification $\times 40$; Scale bars, 20 μ m. **K:** mRNA expression of loricrin, kallikrein 5 (KLK5), involucrin, transglutaminase 1 (TGase1) and filaggrin (FLG) was up-regulated in the *Abca12*^{-/-} neonatal epidermis. (*Abca12*^{-/-} neonates, $n = 5$; wild-type neonates, $n = 5$, mRNA expression levels of wild-type neonatal epidermis = 1). **L:** Western blotting of epidermal extracts showed that protein expression of kallikrein 5 (KLK5) and loricrin was lower in the *Abca12*^{-/-} neonatal epidermis (right) than in the wild-type neonatal epidermis (left). There were no significant differences of desmoglein 1 (DSG1), involucrin, β -actin expressions between the *Abca12*^{-/-} and wild-type epidermis. **M:** Western blotting with anti-profilaggrin/filaggrin antibody revealed the *Abca12*^{-/-} neonatal epidermis (right) expressed more profilaggrin/filaggrin protein than wild-type neonatal epidermis (left). High molecular weight smear band corresponding to non-converted profilaggrin peptides were characteristic to the *Abca12*^{-/-} neonatal epidermis. Western blotting using serial protein dilutions is shown in the supplemental Figure 2 (see Supplemental Figure S2 at <http://ajp.amjpatbol.org>). KLK5, kallikrein 5; LG, lamellar granule; TGase1, transglutaminase 1; CCE, cornified cell envelope; FLG, filaggrin; KHG, keratohyalin granule; DSG1, desmoglein 1; proFLG, profilaggrin; 4FLG, filaggrin tetramer; 3FLG, filaggrin trimer; 2FLG, filaggrin dimer; 1FLG, filaggrin monomer.

tein expression of involucrin or control molecules unconnected with the keratinization process, β -actin, and desmoglein1 (DSG1), between *Abca12*^{-/-} and wild-type neonatal epidermis.

Both *Abca12*^{-/-} and wild-type neonatal skin demonstrated intense profilaggrin/filaggrin expression within granular layer keratinocytes (Figure 2, G and H). However, in

Abca12^{-/-} neonatal skin, profilaggrin/filaggrin distribution was also observed throughout all of the cornified layers (Figure 2H). Western blotting with anti-profilaggrin/filaggrin antibody revealed that neonatal *Abca12*^{-/-} epidermis exhibited a greater amount of profilaggrin/filaggrin protein than that in the neonatal wild-type epidermis (Figure 2M). In particular, high molecular weight smear bands correspond-

ing to unconverted profilaggrin peptides were characteristic of neonatal *Abca12*^{-/-} epidermis. Western blotting using the serial dilutions of protein showed that neonatal *Abca12*^{-/-} epidermis exhibited a filaggrin monomer band, although the ratio of high molecular weight profilaggrin and its derivatives to filaggrin monomer in the *Abca12*^{-/-} neonatal epidermis was extremely high compared with that of the wild-type neonatal epidermis (see Supplemental Figure S2A at <http://ajp.amjpathol.org>). The remaining high molecular bands in the neonatal *Abca12*^{-/-} epidermis indicated defective profilaggrin conversion to filaggrin. Furthermore, we prepared 8 mol/L urea supernatants from precipitated proteins from the *Abca12*^{-/-} neonatal epidermis in RIPA buffer. Western blotting with 8 mol/L urea supernatants confirmed that a proportion of filaggrin monomer, which is insoluble in the RIPA buffer exists in *Abca12*^{-/-} neonatal epidermis (see Supplemental Figure S2B at <http://ajp.amjpathol.org>). In contrast, urea supernatants from precipitated proteins in RIPA buffer of wild-type neonatal epidermis showed only a faint band of filaggrin monomer. This finding indicated that majority of filaggrin monomer in the wild-type neonatal epidermis is soluble in RIPA buffer. These Western blotting results suggested that *Abca12*^{-/-} neonatal epidermis exhibited not only defective profilaggrin/filaggrin conversion but also alteration of filaggrin monomer solubility. We also performed Western blotting with anti-loricrin antibody using 8 mol/L urea supernatant. Using 8 mol/L urea buffer as well as using RIPA buffer the loricrin band was faint in supernatant samples from the *Abca12*^{-/-} neonatal epidermis (data not shown). Thus, the solubility of loricrin was unaltered in the *Abca12*^{-/-} neonatal epidermis and we think that the alteration of solubility in the *Abca12*^{-/-} neonatal epidermis is specific to filaggrin.

Improved Morphological Abnormalities, Corrected Lipid Distribution, and Restored Expression of Differentiation-Specific Molecules in Abca12^{-/-} *Skin Grafts Maintained in Dry Environment*

Since *Abca12*^{-/-} neonates die soon after birth, it was impossible to follow the phenotypic changes in the skin of *Abca12*^{-/-} mice after birth. Therefore, we grafted their skin onto severe combined immunodeficient (SCID) mice and analyzed its morphological and biochemical alterations in the skin after birth/grafting.

Mature grafted *Abca12*^{-/-} skin showed hairless keratotic plates at 3 weeks after transplantation onto the backs of SCID mice (Figure 3, A and B). Light microscopic observations revealed that hair follicles and shafts were buried in keratotic plugs in mature *Abca12*^{-/-} skin (Figure 3, C and D). High power microscopy demonstrated that mature *Abca12*^{-/-} skin showed discernible keratohyalin granules in the granular layers (Figure 3F) that were completely absent in *Abca12*^{-/-} neonatal skin (Figure 1, E and F).

Immunofluorescence staining showed *abca12* staining in wild-type but not *abca12*^{-/-} mice and intense labeling of glucosylceramides/ceramides at the granular/cornified

layer interface in mature grafted *Abca12*^{-/-} skin (Figure 3, I and J), compared with a sparse distribution in the neonatal *Abca12*^{-/-} mouse upper epidermis (Figure 1L). Electron microscopy of mature *Abca12*^{-/-} skin showed many lipid droplets in the granular layer (Figure 3K), although the number of lipid droplets in the cornified layer was reduced when compared with that of neonatal skin (Figure 3L). Using lipid analysis, the amounts of both total ceramides and CER[EOS] were restored in mature *Abca12*^{-/-} epidermis (Figure 3M, and see Supplemental Figure S1, C and D at <http://ajp.amjpathol.org>). These results indicate that mature grafted *Abca12*^{-/-} epidermis was able to obtain a normal ceramide distribution together with a normal composition of ceramides.

Immunolabeling for differentiation-specific molecules confirmed improved keratinization during maturation of the grafted *Abca12*^{-/-} skin (Figure 4, A–J). Intense KLK5 immunolabeling (Figure 4, A and B), *in situ* transglutaminase 1 (TGase1) activity (Figure 4, C and D), and loricrin immunostaining (Figure 4, E and F) were distributed throughout the granular layers in mature grafted *Abca12*^{-/-} skin, compared with a sparse distribution in *Abca12*^{-/-} neonatal skin (Figure 2, B, D, and F). Increased loricrin and KLK5 immunolabeling intensity was confirmed by Western blot analysis using epidermal extracts from mature grafted *Abca12*^{-/-} epidermis (Figure 4K).

Mature grafted *Abca12*^{-/-} skin showed intense profilaggrin/filaggrin labeling in the granular layer (Figure 4H), similar to the mature grafted wild-type skin (Figure 4G). The diffuse profilaggrin/filaggrin distribution throughout the cornified layers observed in *Abca12*^{-/-} neonatal skin (Figure 2H) was not seen in mature grafted *Abca12*^{-/-} skin (Figure 4H). Western blotting with anti-profilaggrin/filaggrin antibody revealed that the normal conversion of profilaggrin to filaggrin was restored in mature *Abca12*^{-/-} epidermis (Figure 4K). Epidermal extracts of mature *Abca12*^{-/-} skin at 3 weeks after transplantation showed low expression of high molecular weight smeared bands and, instead of those, exhibited intense filaggrin monomer bands, compared those with epidermal extracts of *Abca12*^{-/-} neonatal skin.

Analysis of TEWL as a parameter of skin barrier defects, demonstrated *Abca12*^{-/-} that neonatal back skin showed significantly greater TEWL than the wild-type neonatal skin ($n = 3$, $P < 0.001$) (Figure 4L). However, TEWL levels of mature *Abca12*^{-/-} skin 3 weeks after the skin graft were significantly decreased as compared with levels of *Abca12*^{-/-} neonatal skin ($n = 3$, $P < 0.001$).

Subcultured Abca12^{-/-} *Mouse Keratinocytes Attained Normal Lipid Trafficking in the Cytoplasm, with Restoration of Differentiation-Specific Protein Expression and Intact Profilaggrin/Filaggrin Conversion that Was Defective in Primary-Cultured Abca12*^{-/-} *Mouse Keratinocytes*

To verify the results from grafted skin analysis, we performed a similar analysis using primary versus subcultured *Abca12*^{-/-} keratinocytes. Immunolabeling with an-

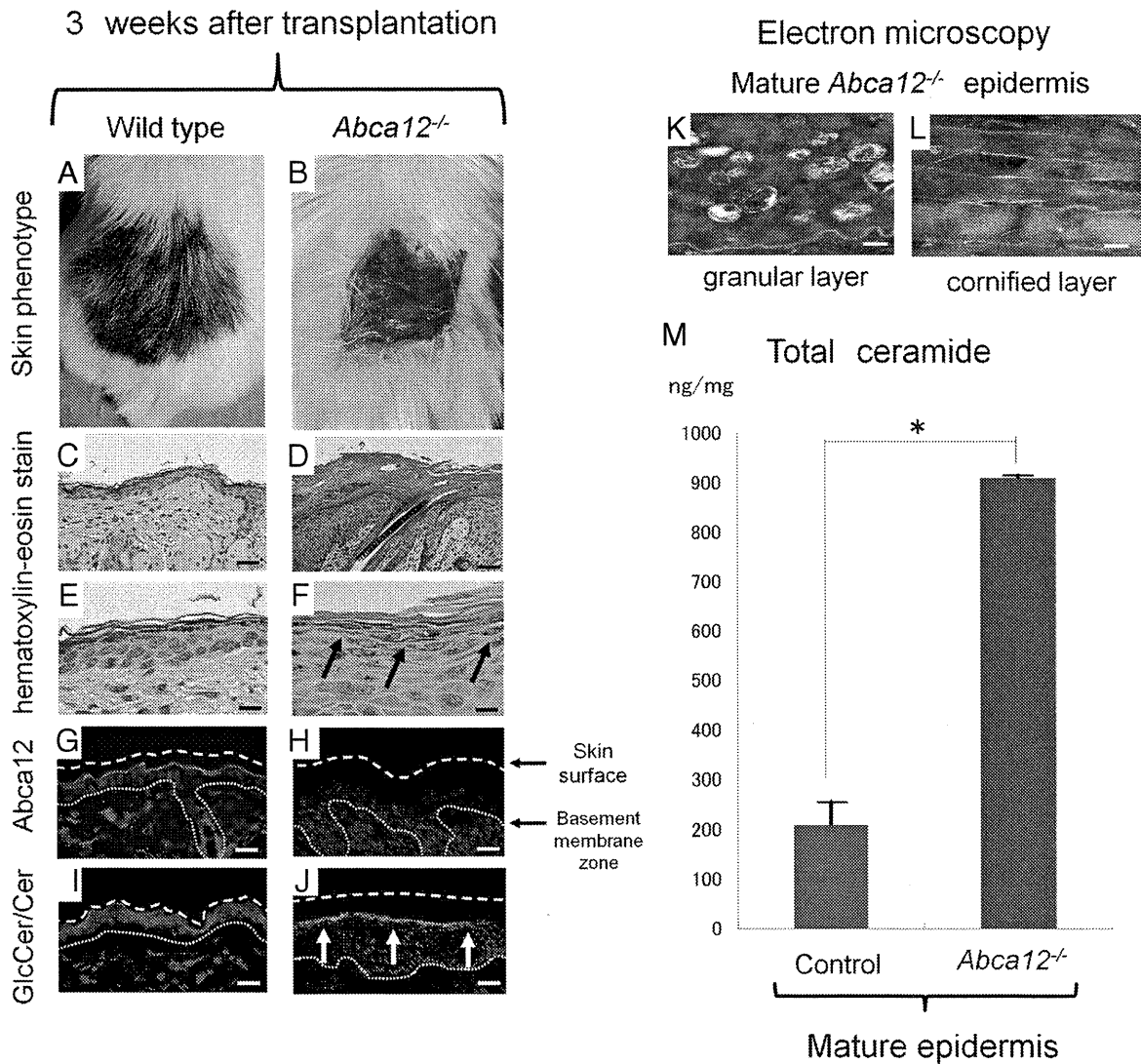


Figure 3. Altered morphology and improvement of ceramide deficiency during maturation of *Abca12^{-/-}* skin. Gross (**A** and **B**) and microscopic (**C–L**) appearances of wild-type and *Abca12^{-/-}* skin three weeks after transplantation onto SCID mice. **A:** Grafted skin of wild-type mice three weeks after transplantation. **B:** Grafted *Abca12^{-/-}* skin three weeks after transplantation showed hairless keratotic plates. **C** and **D:** Light microscopic observation histology (H&E stain; original magnification $\times 40$; Scale bars = 20 μm). Hair follicles and shafts were buried in keratotic plugs in the mature *Abca12^{-/-}* skin three weeks after the skin graft (**D**). **E** and **F:** High power views (H&E stain; original magnification $\times 60$; Scale bars = 10 μm). Mature *Abca12^{-/-}* skin three weeks after transplantation showed discernible keratohyalin granule in the granular layers (**F**, arrows) that were lacked in *Abca12^{-/-}* neonatal skin (see Figure 1, D and F). **G** and **H:** By immunofluorescence staining, Abca12 expression (Alexa488, green) was detected in the mature wild-type mouse skin (**G**), but not in the mature *Abca12^{-/-}* skin (**H**). **I** and **J:** Immunofluorescence staining showed an intense distribution of glucosylceramide/ceramide (GlcCer/Cer) (Alexa 488, green) at the granular/cornified layer interface in mature *Abca12^{-/-}* epidermis (**J**, arrows), compared with a sparse distribution in the neonatal *Abca12^{-/-}* mouse upper epidermis (see Figure 1J). **K** and **L:** Ultrastructural observation of the grafted *Abca12^{-/-}* skins three weeks after transplantation. There were many lipid droplets in the granular layer (**K**, red arrowheads), however the number of lipid droplets in the cornified layer (**L**, red arrowheads) was fewer than that of the neonatal *Abca12^{-/-}* skin (see Figure 1F). Original magnification: $\times 10000$ (**K**), $\times 5000$ (**L**); Scale bars: 100 nm (**K**), 200 nm (**L**). **M:** From the lipid analysis of grafted skins, total ceramides levels of mature *Abca12^{-/-}* epidermis were restored. (*Abca12^{-/-}* grafted skins, $n = 2$; control grafted skins, $n = 2$) ($*P < 0.01$). GlcCer, glucosylceramide; Cer, ceramide

ti-glucosylceramide/ceramide antibody demonstrated a congested glucosylceramide/ceramide pattern in differentiated primary-cultured *Abca12^{-/-}* mouse keratinocytes after first passage (Figure 5, B and E), compared with an uncongested, diffuse peripheral glucosylceramide/ceramide pattern in differentiated primary-cultured wild-type mouse keratinocytes (Figure 5, A and D). After 10 passages, subcultured *Abca12^{-/-}* keratinocytes showed a widely distributed, diffuse glucosylceramide/ceramide staining pattern, similar to those of primary-cultured wild-type keratinocytes (Figure 5, C and F). Subcultured wild-type keratinocytes after 10 passages failed

to show any alterations in lipid distribution (data not shown). These results indicate that lipid trafficking recovered during 10 passages of subculture in our *Abca12^{-/-}* keratinocytes.

To investigate this altered differentiation state of primary/subcultured *Abca12^{-/-}* keratinocytes, we performed real-time RT-PCR and immunoblot analysis (Figure 5, G and H). No significant differences were obtained in lorincrin, KLK5, involucrin, TGase1 and filaggrin mRNA expression between primary-cultured *Abca12^{-/-}* and wild-type keratinocytes (Figure 5G). Subcultured *Abca12^{-/-}* keratinocytes showed higher lorincrin, KLK5 and TGase1 mRNA

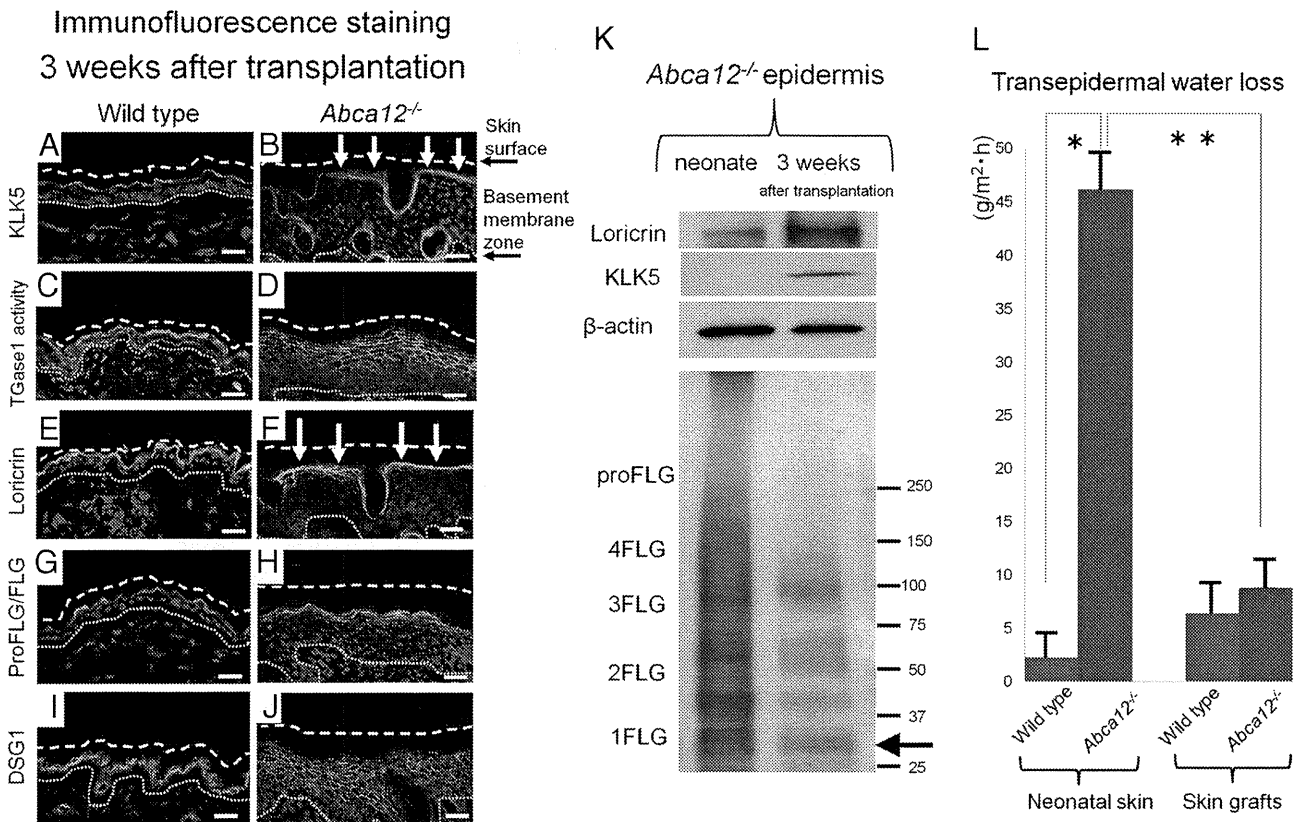


Figure 4. Improvement of previously disrupted differentiation-specific protein expression and defective skin barrier function in postnatal *Abca12*^{-/-} skin. **A–J:** Immunolabeling for differentiation-specific molecules confirmed improved keratinization during maturation of the grafted *Abca12*^{-/-} skin. Intense kallikrein 5 (KLK5) immunostaining (**A** and **B**, white arrows), *in situ* transglutaminase 1 (TGase1) activity labeling (**C** and **D**) and loricrin immunolabeling (**E** and **F**, white arrows) were seen throughout the granular layers in mature grafted *Abca12*^{-/-} skin, compared with their sparse distribution in the *Abca12*^{-/-} neonatal skin (see Figure 2, B, D and F). Increased loricrin and KLK5 immunolabeling intensity was confirmed by Western blot analysis using epidermal extracts from mature grafted *Abca12*^{-/-} skin (**K**). Mature grafted *Abca12*^{-/-} skin showed intense profilaggrin/filaggrin labeling in the granular layer (**H**), similar to the mature grafted wild-type skin (**G**). Diffuse profilaggrin/filaggrin staining in the entire cornified layers observed in *Abca12*^{-/-} neonatal skin (see Figure 2H) disappeared in mature grafted *Abca12*^{-/-} skin. Expression of desmoglein 1 (DSG1), unassociated with keratinization, was not altered in the grafted skin (**I** and **J**). Western blotting with anti-profilaggrin/filaggrin antibody revealed that normal conversion of profilaggrin to filaggrin was restored in mature *Abca12*^{-/-} epidermis (**K**). Nuclear stain: propidium iodide, red; original magnification $\times 40$; Scale bars = 20 μm . **L:** The barrier function in the transplanted skin was assessed by measuring transepidermal water loss (TEWL). The *Abca12*^{-/-} neonates (red bar, left) showed significantly greater TEWL than the wild-type neonates (blue bar, left) showed ($*P < 0.001$). TEWL levels of mature *Abca12*^{-/-} epidermis three weeks after the skin graft (red bar, right) were significantly decreased as compared with levels of *Abca12*^{-/-} neonatal skin (red bar, left) ($**P < 0.001$), and was similar to levels of mature wild-type skin three weeks after the skin graft (blue bar, right). (*Abca12*^{-/-} neonates, $n = 3$; wild-type neonates, $n = 3$; mature *Abca12*^{-/-} skin, $n = 3$; mature wild-type skin, $n = 3$). KLK5, kallikrein 5; proFLG, profilaggrin; FLG, filaggrin; 4FLG, filaggrin tetramer; 3FLG, filaggrin trimer; 2FLG, filaggrin dimer; 1FLG, filaggrin monomer.

levels compared with primary-cultured *Abca12*^{-/-} keratinocytes (Figure 5G). Blot extracts from differentiated primary-cultured *Abca12*^{-/-} keratinocytes showed low expression of loricrin and KLK5 (Figure 5H), as observed in neonatal *Abca12*^{-/-} mice epidermis (Figure 2L). However, extracts from subcultured *Abca12*^{-/-} keratinocytes showed restoration of loricrin and KLK5 expression (Figure 5H), as observed in grafted mice epidermis (Figure 4K).

Western blotting with anti-profilaggrin/filaggrin antibody revealed that the filaggrin expression pattern had become normalized in subcultured *Abca12*^{-/-} keratinocytes (Figure 5H). Cell lysates from 10 passage-subcultured *Abca12*^{-/-} keratinocytes showed an intense filaggrin monomer band that was faint in lysates from *Abca12*^{-/-} primary first-passage keratinocytes.

Studies of subcultured *Abca12*^{-/-} keratinocytes demonstrated restored differentiation, at least in part, similar to that observed in mature *Abca12*^{-/-} skin grafts.

cDNA Microarray Analysis Revealed Up-Regulation of 22 Lipid Metabolic and/or Transport-Related Genes

To investigate the mechanism of restoration of intact keratinocytes differentiation in subcultured *Abca12*^{-/-} keratinocytes, we analyzed whole gene expression profile of primary/subcultured *Abca12*^{-/-} keratinocytes maintained under high Ca^{2+} condition using cDNA microarray methods. We obtained the 35,582 gene expression profile and observed 566 transcripts that were up-regulated more than three-fold in subcultured *Abca12*^{-/-} keratinocytes compared with primary-cultured *Abca12*^{-/-} keratinocytes. Among them, we searched for genes related to "lipid metabolism and/or lipid transporter function," and identified 22 specific transcripts including solute carrier family 22 member 7 (*Slc22a7*), prostaglandin D2 syn-

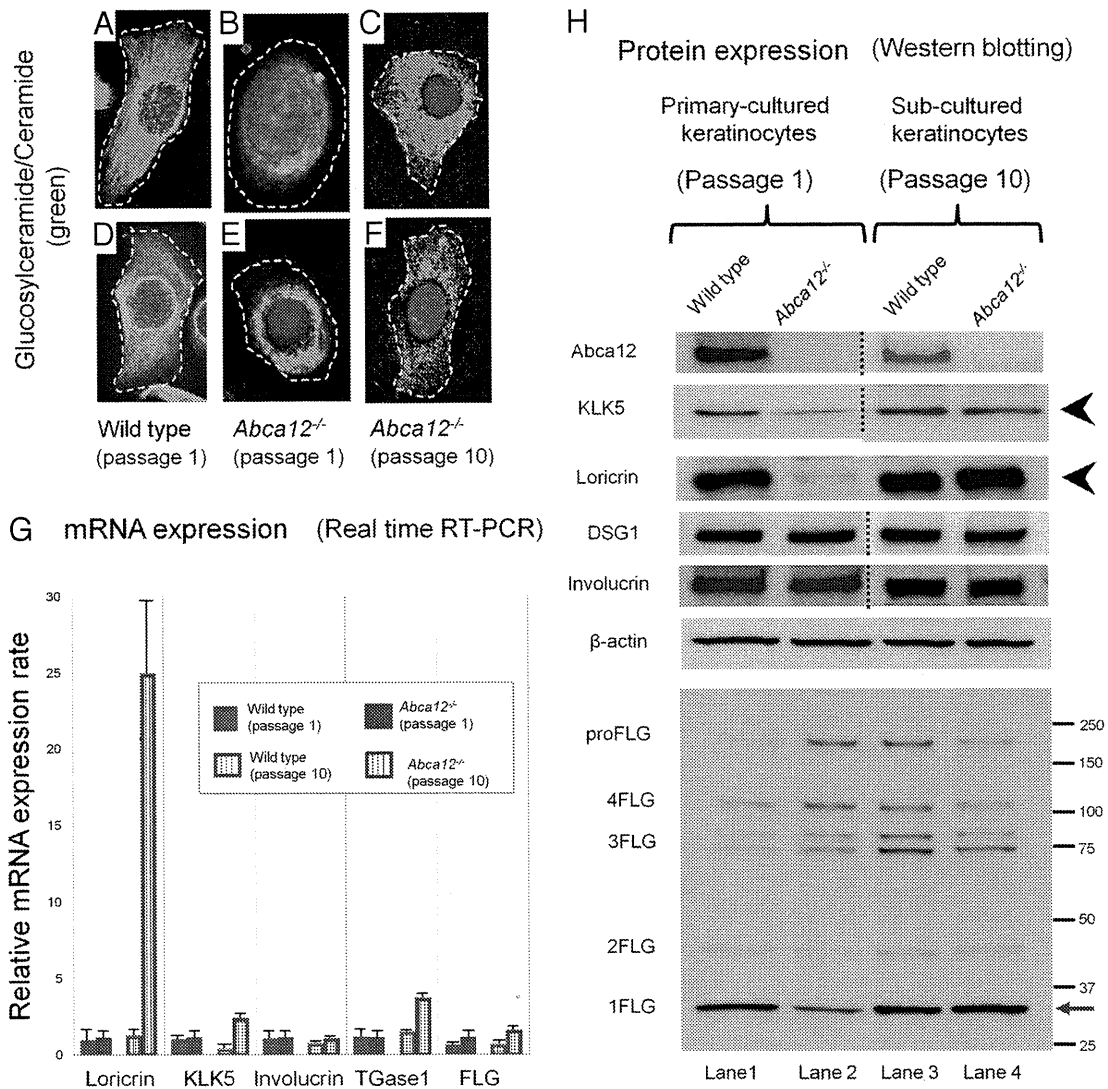


Figure 5. Subcultured *Abca12*^{-/-} mouse keratinocytes exhibited restored intracytoplasmic localization of glucosylceramide/ceramide, protein expression of differentiation-specific molecules and profilaggrin conversion. **A–F:** Intracytoplasmic localization of glucosylceramide/ceramide in cultured keratinocytes. Immunolabeling demonstrated a congested pattern of glucosylceramide/ceramide (Alexa 488, green) in differentiated primary-cultured *Abca12*^{-/-} mouse keratinocytes after first passage (**B** and **E**), in contrast with the uncongested, diffuse, peripheral pattern in the differentiated keratinocytes of a wild-type mouse (**A** and **D**). After 10 passages, subcultured *Abca12*^{-/-} keratinocytes showed a widely distributed, diffuse glucosylceramide staining pattern (**C** and **F**), similar to those of wild-type keratinocytes. Subcultured wild-type keratinocytes after ten passages did not show any alterations in lipid distribution (data not shown). Nuclear stain: propidium iodide, red; original magnification $\times 60$. **Dotted lines** are the cell surface. **G:** There were no significant differences in loricrin, kallikrein 5 (KLK5), involucrin, transglutaminase 1 (TGase1), and filaggrin (FLG) mRNA expression between primary-cultured *Abca12*^{-/-} keratinocytes (red bars, left) and primary-cultured wild-type keratinocytes (blue bars, left). Subcultured *Abca12*^{-/-} keratinocytes (red bars, right) showed higher mRNA levels of loricrin, kallikrein 5, and transglutaminase 1 compared with primary-cultured *Abca12*^{-/-} keratinocytes (red bars, left) and subcultured wild-type keratinocytes (blue bars, right). No significant difference was observed in involucrin and filaggrin mRNA expression. (primary-cultured *Abca12*^{-/-}, $n = 5$; primary-cultured wild-type, $n = 5$; subcultured *Abca12*^{-/-}, $n = 5$; subcultured wild-type, $n = 5$, mRNA expression levels of *Abca12*^{-/-} primary cultured keratinocytes = 1). **H:** Western blotting of differentiated cultured keratinocytes lysates under high Ca^{2+} condition showed that loricrin and KLK5 expression was lower in *Abca12*^{-/-} primary-cultured keratinocytes (**lane 2**) than that of the wild-type primary-cultured keratinocytes (**lane 1**). Extracts from subcultured *Abca12*^{-/-} keratinocytes showed restoration of loricrin and KLK5 expression (**lane 4**, **black arrowheads**). Western blotting with anti-profilaggrin/filaggrin antibody revealed that the *Abca12*^{-/-} primary-cultured keratinocytes (**lane 2**) had reduced expression of mature filaggrin monomer than the wild-type primary-cultured keratinocytes (**lane 1**). In addition, the lysate from *Abca12*^{-/-} primary-cultured keratinocytes exhibited plenty of high molecular weight bands, which indicated profilaggrin expression (**lane 2**). The filaggrin expression pattern was normalized in subcultured *Abca12*^{-/-} keratinocytes (**lane 4**). Cell lysates from subcultured *Abca12*^{-/-} keratinocytes showed an intense filaggrin monomer band that was faint in lysates from *Abca12*^{-/-} primary first-passage keratinocytes (**lane 2** and **4**, **red arrow**). KLK5, kallikrein 5; TGase, transglutaminase; DSG1, desmoglein 1; proFLG, profilaggrin; 4FLG, filaggrin tetramer; 3FLG, filaggrin trimer; 2FLG, filaggrin dimer; 1FLG, filaggrin monomer.

thetase (*Ptgs2*), annexin A9 (*Anxa9*), bactericidal/permeability-increasing protein-like 2 (*Bpil2*), phosphatidylethanolamine binding protein-2 variant 1 homolog (*Pbp2*), lipocalin 7 (*Tinagl*), *Gpr119*, solute carrier family 5 member 1 (*Slc5a1*), prostaglandin- endoperoxide synthase 2

(*Ptgs2*), and solute carrier family 30 member 1 (*Slc30a1*) (see Supplemental Table S1 at <http://ajp.amjpathol.org>). Notably, these genes included four ATP-binding transporter family members: *Abca17*, *Abca1a*, *Abcc5*, and *Abcb11* that were up-regulated at least three-fold.

Keratinocytes Treated with Retinoids Failed to Exhibit Normal Differentiation and Therapeutic Trials onto Grafted HI Model Mice Failed to Demonstrate Skin Phenotype Recovery

As treatment trials for primary keratinocytes, Western blotting revealed that primary-cultured wild-type keratinocytes expressed a large amount of loricrin peptide and had a decent amount of filaggrin monomer converted from profilaggrin (see Supplemental Figure S3 at <http://ajp.amjpathol.org>). Both isotretinoin (10^{-6} mol/L) and etretinate (10^{-6} mol/L) in the cultured medium for 48 hours lead to remarkable reduction of loricrin protein expression in primary-cultured wild-type keratinocytes, although filaggrin expression patterns were not altered. Neither isotretinoin (10^{-6} mol/L) nor etretinate (10^{-6} mol/L) improved the deficient loricrin protein expression or defective profilaggrin conversion in the primary-cultured *Abca12*^{-/-} keratinocytes under high Ca²⁺ condition.

As a treatment trial for HI grafted skin, oral administration of various doses of isotretinoin (1 or 10 mg/kg daily for 10 consecutive days) to HI skin graft-recipient SCID mice demonstrated no change in the skin phenotype of grafted HI model mice skin at all (data not shown).

Discussion

Keratinocyte terminal differentiation (keratinization) is remarkably important to skin physiology and essential for epidermal function including barrier formation. Keratinization is a highly regulated process, involving a number of genes and pathways. Until now, abnormalities in keratinocyte differentiation have been reported in HI patients. Morphologically, Buxman et al¹⁰ have reported that granular layers were absent or poorly formed in HI patient epidermis. Dale et al reported abnormal lamellar granules and defective profilaggrin conversion both in HI patients skin and their cultured keratinocytes.¹¹ Profilaggrin conversion to filaggrin is a key step during epidermal keratinization. Fleckman et al¹² reported that HI keratinocytes in 3 dimensional culture were unable to show the adequate differentiated epithelium and profilaggrin/filaggrin conversion. Recently, Thomas et al reported that the desquamation specific enzyme, kallikrein 5, and cathepsin D, were remarkably reduced in HI model skin using ABCA12 small interfering RNA knockdown keratinocytes.¹³

In the present study, we have demonstrated that keratinocyte differentiation was severely disrupted in both *Abca12*^{-/-} HI neonatal model mouse skin and primary-cultured *Abca12*^{-/-} keratinocytes. The present findings were consistent with previous reports of findings in HI patient's skin. Our neonatal HI model mice skin showed no apparent keratohyalin granules within any of their granular layer cells, which was consistent with Buxman's study.¹⁰ Furthermore, our immunoblotting results confirmed defective profilaggrin/filaggrin conversion, which was consistent with the studies by Dale et al¹¹ and Fleckman et al.¹² Our immunostaining and immunoblotting results showed reduced expression of KLK5 in neonatal

Abca12^{-/-} epidermis and primary-cultured *Abca12*^{-/-} keratinocytes, which was consistent with the study by Thomas et al.¹³ We therefore believe that our *Abca12*^{-/-} HI model mouse faithfully reproduces the molecular condition thus far identified in human HI epidermis in addition to mimicking clinical phenotype.⁵

Zuo et al⁶ suggested that loss of ABCA12 did not induce a block in the normal processing of profilaggrin to filaggrin in another reported ABCA12 deficient mouse strain, although the solubility of filaggrin was altered. We believe that our data are consistent with Zuo's study. In the present study, we showed high molecular weight bands in RIPA buffer extracted supernatant from neonatal *Abca12*^{-/-} epidermis. In study by Zuo et al,⁶ similar high molecular weight bands were also seen by the Western blotting after detergent buffer supernatant extraction. We also showed an alteration in filaggrin monomer solubility using 8 mol/L urea supernatant, reproducing the findings of Zuo et al.⁶ The major difference between these two studies is that Zuo et al⁶ showed no filaggrin monomer band after detergent buffer supernatant extraction in their ABCA12 deficient mouse skin. In contrast, we detected filaggrin monomer band in RIPA supernatant of our *Abca12*^{-/-} neonatal epidermis. This finding might result from differences in lysis buffer, tissue sample

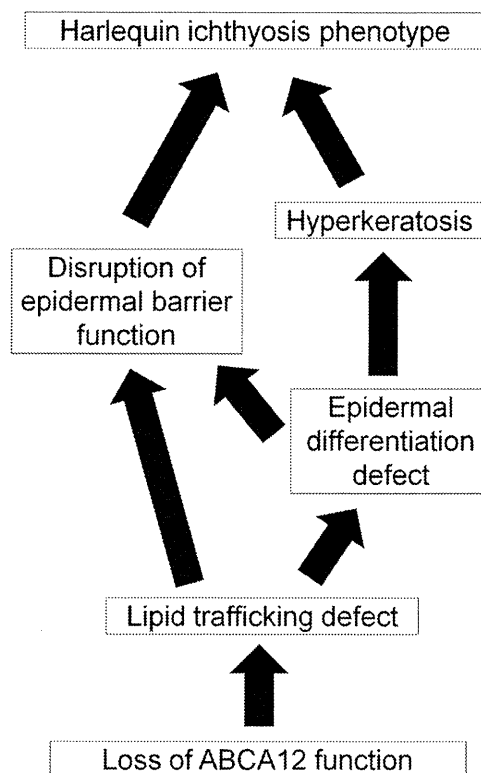


Figure 6. Putative pathomechanism of harlequin ichthyosis. Based on our results, we propose a novel pathogenetic mechanism underlying harlequin ichthyosis (HI). Our results suggested that a lipid trafficking defect due to loss of ABCA12 function leads to not only malformation of the epidermal lipid barrier but also “an epidermal differentiation defect.” In our hypothesis, the severe hyperkeratosis, a characteristic phenotype of HI skin, is not a hyperkeratosis compensating for any barrier insufficiency, but a hyperkeratosis due to both defective differentiation and an abnormal desquamation process. The present scenario explains both the HI skin phenotype at/after birth and even *in utero*.

(whole skin or only epidermis), or harvest time (E18.5 or neonate). We conclude that neonatal *Abca12*^{-/-} epidermis exhibits not only defective profilaggrin/filaggrin conversion but also alterations in filaggrin monomer solubility, as previously suggested by Dale et al,¹¹ Fleckman et al,¹² and Zuo et al.⁶

Based on our results, we propose several new pathogenetic mechanisms for HI (Figure 6). Our results suggest that “an epidermal differentiation defect” is the major pathomechanism in HI. This new pathogenesis model is furthermore able to resolve the conflicting “the barrier insufficiency” theory with the (human) HI clinical phenotype. Our novel “epidermal differentiation” theory can explain HI skin phenotype at birth and even *in utero*. In our theory, severe hyperkeratosis, characteristic of the HI skin phenotype, was not a compensative hyperkeratosis for barrier insufficiency, but a hyperkeratosis due to defective differentiation and desquamation processes.

Epidermal differentiation defects in our HI model mice suggest that ABCA12 lipid trafficking, which occurs during the early stages of keratinization, is a crucial step for correct keratinocyte terminal differentiation. In normal granular layer keratinocytes, ABCA12 transports lipids and forms lamellar granules.³ Just after the extrusion of lipids from lamellar granules at the granular/cornified layer interface, loricrin accumulates at the cell periphery and is integrated into the insoluble cornified cell envelope by transglutaminases.¹⁴ At the final phase of terminal differentiation, profilaggrin undergoes many post-translational modifications, including conversion to functional filaggrin monomers, which aid in the bundling of keratin intermediate filaments and formation of the cornified cell envelope.¹⁴⁻¹⁶ Serine proteases including KLK5 are involved in the desquamation process after keratinization.¹⁷ Our present results suggest that defective lipid trafficking and lamellar granule formation fail to initiate the normal sequence of events of the keratinization process. These facts indicate that ABCA12 lipid trafficking is essential to precisely regulate keratinocyte differentiation.

Interestingly, mature grafted HI model mouse skin and subcultured *Abca12*^{-/-} keratinocytes showed improvement in the *Abca12*^{-/-}-related abnormalities observed in neonatal skin and primary-cultured keratinocytes, such as the aberrant ceramide distribution, reduced differentiation-specific protein expression and profilaggrin/filaggrin conversion defects. Similar to our *Abca12*^{-/-} model mouse skin, improvement in skin manifestations during maturation was observed in several other ichthyotic model mice. Loricrin knockout mice exhibit shiny translucent skin at birth although these mice showed a normal skin phenotype at 4 to 5 days after birth.¹⁸ Biochemically, the mice showed increased protein expression of small proline rich proteins, which are also cornified cell envelope components during skin maturation.¹⁸ Mature 12R-lipoxygenase knockout mouse skin showed recovery of skin barrier function and restoration of profilaggrin conversion after maturation, which had been lacking in the neonatal mice.^{19,20} In addition, mature transglutaminase 1 knockout mouse skin also showed skin barrier functional recovery, although exact compensation mechanisms other than hyperkeratosis were not identified.²¹

To find any clues for the mechanism of compensation in *Abca12*^{-/-} mice, we conducted cDNA microarray analysis. We could find that several transporters including four ATP-binding cassette (ABC) transporter family genes were up-regulated in subculture compared with primary-cultured *Abca12*^{-/-} keratinocytes. We consider these up-regulated ABC transporters as prime candidate genes to compensate for the loss of ABCA12 function. These lipid transport/metabolism-related molecules might help in lipid trafficking and/or recovery of epidermal differentiation in *Abca12*^{-/-} keratinocytes.

The recovery of skin barrier function and self-improvement of epidermal differentiation defects in mature *Abca12*^{-/-} skin gave us important clues to aid in treatment of HI patients. Infants affected with HI frequently die within the neonatal period, although the survival rate of HI newborns has increased recently with the arrival of neonatal intensive care regimes with retinoid administration.²²⁻²⁶ Our observations in mature *Abca12*^{-/-} skin further confirmed that the early neonatal period is a critical time defining the prognosis. In this context, neonatal intensive care for HI newborns in the initial neonatal period is important for their survival.

We had already tried systemic retinoid administration to pregnant mice as a fetal therapy, although neither improvement of the skin manifestations nor extension of the survival period was obtained in the *Abca12*^{-/-} newborns from the treated-mother mice.⁵ Based on the clinical efficacy of retinoids to HI patients,²²⁻²⁶ we conducted retinoid administration to the primary-cultured *Abca12*^{-/-} keratinocytes. We could not detect any recovery of differentiation defects in the primary-cultured *Abca12*^{-/-} keratinocytes treated with retinoids. These results of our therapeutic trials to fetuses in the previous report⁵ and to primary keratinocytes in this study indicated that retinoids may be ineffective for modifying the epidermal differentiation defects during the fetal period. These facts were consistent with the known effects of retinoids, which enhance proliferation and suppress differentiation of keratinocytes.^{27,28} Further, we performed a treatment trial on grafted SCID mice using systemic isotretinoin administration. Oral administration of any dose of isotretinoin (either 1 or 10 mg/kg daily, for 10 consecutive days) to the HI-skin-grafted SCID mice failed to improve the skin phenotype of grafted HI skin at all. We failed to obtain any clue to understand the reason why retinoids are only effective for HI patients from our present study.

In conclusion, we have demonstrated that disrupted epidermal keratinocyte differentiation is the pathomechanism involved in HI, and that during maturation, *Abca12*^{-/-} epidermal keratinocytes regain normal keratinocyte differentiation. This restoration of differentiation is likely to be associated with the skin phenotype improvement observed in HI survivors.

Acknowledgment

We thank Dr. James R. McMillan for proofreading this manuscript.

References

1. Akiyama M: Pathomechanisms of harlequin ichthyosis and ABCA transporters in human diseases. *Arch Dermatol* 2006, 142:914–918
2. Hovnanian A: Harlequin ichthyosis unmasked: a defect of lipid transport. *J Clin Invest* 2005, 115:1708–1710
3. Akiyama M, Sugiyama-Nakagiri Y, Sakai K, McMillan JR, Goto M, Arita K, Tsuji-Abe Y, Tabata N, Matsuoka K, Sasaki R, Sawamura D, Shimizu H: Mutations in lipid transporter ABCA12 in harlequin ichthyosis and functional recovery by corrective gene transfer. *J Clin Invest* 2005, 115:1777–1784
4. Kelsell DP, Norgett EE, Unsworth H, Teh MT, Cullup T, Mein CA, Dopping-Hepenstal PJ, Dale BA, Tadini G, Fleckman P, Stephens KG, Sybert VP, Mallory SB, North BV, Witt DR, Sprecher E, Taylor AE, Ilchyshyn A, Kennedy CT, Goodyear H, Moss C, Paige D, Harper JI, Young BD, Leigh IM, Eady RA, O'Toole EA: Mutations in ABCA12 underlie the severe congenital skin disease harlequin ichthyosis. *Am J Hum Genet* 2005, 76:794–803
5. Yanagi T, Akiyama M, Nishihara H, Sakai K, Nishie W, Tanaka S, Shimizu H: Harlequin ichthyosis model mouse reveals alveolar collapse and severe fetal skin barrier defects. *Hum Mol Genet* 2008, 17:3075–3083
6. Zuo Y, Zhuang DZ, Han R, Isaac G, Tobin JJ, McKee M, Welti R, Brissette JL, Fitzgerald ML, Freeman MW: ABCA12 maintains the epidermal lipid permeability barrier by facilitating formation of ceramide linoleic esters. *J Biol Chem* 2008, 283:36624–36635
7. Akiyama M, Smith LT, Shimizu H: Expression of transglutaminase activity in developing human epidermis. *Br J Dermatol* 2000, 142:223–225
8. Raghunath M, Hennies HC, Velten F, Wiebe V, Steinert PM, Reis A, Traupe H: A novel in situ method for the detection of deficient transglutaminase activity in the skin. *Arch Dermatol Res* 1998, 290:621–627
9. Masukawa Y, Narita H, Shimizu E, Kondo N, Sugai Y, Oba T, Homma R, Ishikawa J, Takagi Y, Kitahara T, Takema Y, Kita K: Characterization of overall ceramide species in human stratum corneum. *J Lipid Res* 2008, 49:1466–1476
10. Buxman MM, Goodkin PE, Fahrenbach WH, Dimond RL: Harlequin ichthyosis with epidermal lipid abnormality. *Arch Dermatol* 1979, 115:189–193
11. Dale BA, Holbrook KA, Fleckman P, Kimball JR, Brumbaugh S, Sybert VP: Heterogeneity in harlequin ichthyosis, an inborn error of epidermal keratinization: variable morphology and structural protein expression and a defect in lamellar granules. *J Invest Dermatol* 1990, 94:6–18
12. Fleckman P, Hager B, Dale BA: Harlequin ichthyosis keratinocytes in lifted culture differentiate poorly by morphologic and biochemical criteria. *J Invest Dermatol* 1997, 109:36–38
13. Thomas AC, Tattersall D, Norgett EE, O'Toole EA, Kelsell DP: Premature terminal differentiation and a reduction in specific proteases associated with loss of ABCA12 in Harlequin ichthyosis. *Am J Pathol* 2009, 174:970–978
14. Bickenbach JR, Greer JM, Bundman DS, Rothnagel JA, Roop DR: Loricrin expression is coordinated with other epidermal proteins and the appearance of lipid lamellar granules in development. *J Invest Dermatol* 1995, 104:405–410
15. Candi E, Schmidt R, Melino G: The cornified envelope: a model of cell death in the skin. *Nat Rev Mol Cell Biol* 2005, 6:328–340
16. Denecker G, Ovaere P, Vandenabeele P, Declercq W: Caspase-14 reveals its secrets. *J Cell Biol* 2008, 180:451–458
17. Meyer-Hoffert U, Wu Z, Schroder JM: Identification of lympho-epithelial Kazal-type inhibitor 2 in human skin as a kallikrein-related peptidase 5-specific protease inhibitor. *PLoS One* 2009, 4:e4372
18. Koch PJ, de Viragh PA, Scharer E, Bundman D, Longley MA, Bickenbach J, Kawachi Y, Suga Y, Zhou Z, Huber M, Hohl D, Kartasova T, Jarnik M, Steven AC, Roop DR: Lessons from loricrin-deficient mice: compensatory mechanisms maintaining skin barrier function in the absence of a major cornified envelope protein. *J Cell Biol* 2000, 151:389–400
19. Epp N, Furstenberger G, Muller K, de Juanes S, Leitges M, Hausser I, Thieme F, Liebisch G, Schmitz G, Krieg P: 12R-lipoxygenase deficiency disrupts epidermal barrier function. *J Cell Biol* 2007, 177:173–182
20. de Juanes S, Epp N, Latzko S, Neumann M, Furstenberger G, Hausser I, Stark HJ, Krieg P: Development of an Ichthyosiform Phenotype in Alox12b-Deficient Mouse Skin Transplants. *J Invest Dermatol* 2009, 129:1429–1436
21. Kuramoto N, Takizawa T, Takizawa T, Matsuki M, Morioka H, Robinson JM, Yamanishi K: Development of ichthyosiform skin compensates for defective permeability barrier function in mice lacking transglutaminase 1. *J Clin Invest* 2002, 109:243–250
22. Prasad RS, Pejaver RK, Hassan A, Dusari S, Wooldridge MA: Management and follow-up of harlequin siblings. *Br J Dermatol* 1994, 130:650–653
23. Lawlor F, Peiris S: Harlequin fetus successfully treated with etretinate. *Br J Dermatol* 1985, 112:585–590
24. Ward PS, Jones RD: Successful treatment of a harlequin fetus. *Arch Dis Child* 1989, 64:1309–1311
25. Haftek M, Cambazard F, Dhouailly D, Reano A, Simon M, Lachaux A, Serre G, Claudy A, Schmitt D: A longitudinal study of a harlequin infant presenting clinically as non-bullous congenital ichthyosiform erythroderma. *Br J Dermatol* 1996, 135:448–453
26. Singh S, Bhura M, Maheshwari A, Kumar A, Singh CP, Pandey SS: Successful treatment of harlequin ichthyosis with acitretin. *Int J Dermatol* 2001, 40:472–473
27. Eichner R, Kahn M, Capetola RJ, Gendimenico GJ, Mezick JA: Effects of topical retinoids on cytoskeletal proteins: implications for retinoid effects on epidermal differentiation. *J Invest Dermatol* 1992, 98:154–161
28. Eichner R: Epidermal effects of retinoids: in vitro studies. *J Am Acad Dermatol* 1986, 15:789–797

Neutral Lipid Storage Leads to Acylceramide Deficiency, Likely Contributing to the Pathogenesis of Dorfman–Chanarin Syndrome

Journal of Investigative Dermatology (2010) **130**, 2497–2499; doi:10.1038/jid.2010.145; published online 3 June 2010

TO THE EDITOR

Dorfman–Chanarin syndrome (DCS) is an autosomal recessive, neutral lipid storage disorder with ichthyosis (NLSDI) due to loss-of-function mutations in *CGI-58* (α/β -hydrolase domain-containing protein 5, *ABHD5*). *CGI-58* encodes a 39 kDa protein, a widely expressed cofactor in mammalian tissues including epidermis that activates adipose triglyceride (TG) lipase (reviewed in Schweiger *et al.*, 2009; Yamaguchi and Osumi, 2009), as well as other still unidentified TG lipases (Radner *et al.*, 2009). *CGI-58* expression increases during keratinocyte differentiation; and conversely, knock-down of this cofactor reduces keratinocyte differentiation (Akiyama *et al.*, 2008). Epidermal permeability barrier defects due in part to lamellar/nonlamellar phase separation of secreted lipids, within extracellular domains of the stratum corneum (SC) have been proposed to account for the barrier abnormalities in NLSDI (Elias and Williams, 1985; Demerjian *et al.*, 2006). Although defective extracellular lipid organization clearly is one contributor (Demerjian *et al.*, 2006), we assessed whether diversion of free fatty acid (FA) into esterified lipids causes lipid abnormalities that further impact barrier formation.

We recently reported a DCS patient with a, to our knowledge, previously unreported *CGI-58* missense mutation (Ujihara *et al.*, 2010), exhibiting abnormal barrier-related structures resembling other NLSDI patients (Demerjian

et al., 2006). Both mild and severely affected ichthyotic SCs revealed increased TG and decreased FA levels in comparison with SC fraction from normal subjects (Ujihara *et al.*, 2010). Pertinently, the extent of the increase in TG levels correlated with site-specific differences in the severity of the dermatosis (Ujihara *et al.*, 2010). These observations suggest that divergence of FA to TG contributes to disease phenotype in NLSDI.

We previously showed that ω -O-acylceramides (or acylCer) that have only been identified in differentiated layers of epidermis in terrestrial mammals are essential constituents of the epidermal permeability barrier; that is, lack of acylCer formation results in neonatal death due to abnormal epidermal permeability barrier function (Vasireddy *et al.*, 2007). AcylCer and the de- ω -O-esterified form (ω -hydroxy [ω -OH] ceramide [Cer]) are present either as free (unbound) or bound species (Uchida and Holleran, 2008). The latter form a continuous lipid monolayer, the corneocyte-bound lipid envelope (CLE); that is, a pool of ω -OH Cer, which is covalently bound to the external surface of the cornified envelope (Uchida and Holleran, 2008). Although free acylCer are critical for the formation of the lamellar membranes (Bouwstra *et al.*, 1998), our previous studies suggest the CLE is also important for normal permeability barrier function (Behne *et al.*, 2000). Prior studies suggest that FAs derived from TG are used in the

ω -O-esterification step to form acylCer (Wertz and Downing, 1990). Moreover, TG, linoleate, and acylCer, but not phosphoglycerolipid content, decline in acyl-CoA: diacylglycerol acyltransferase-2-deficient mice, which also show a permeability barrier abnormality (Stone *et al.*, 2004). In addition, linoleate, which is the predominant FA that is used for ω -O-esterification, is enriched in TG in mouse skin (Stone *et al.*, 2004). Thus, we hypothesized that a failure of TG hydrolysis, due to abnormal *CGI-58* function, could attenuate permeability barrier formation in NLSDI by decreasing acylCer content of affected SC.

Therefore, we first investigated the lipid profiles in solvent extracts of SC from this DCS patient (Ujihara *et al.*, 2010). Neither cholesterol (Ujihara *et al.*, 2010) nor total (bulk) Cer (Figure 1a) content was altered. Yet, Cer comprises a family of at least 10 species in humans (Uchida and Holleran, 2008). Because not only bulk Cer amount but also each individual Cer species contributes to the formation of competent lamellar structures required for barrier function (Bouwstra *et al.*, 1998), we subfractionated Cer into individual Cer species. Whereas the major Cer subfractions, NS (Cer 2), NP (Cer 3), and AS (Cer 5) were not significantly altered, acylCer were present at only trace levels in the patient sample (Figure 1b; because sample amounts were limited, other minor Cer species; that is, EOH (Cer 4), AP (Cer 6) (AP), AH (Cer 7) could not be quantitated) (abbreviations for Cer structures are according to Motta *et al.* and Robson K. *et al.*, details reviewed in Uchida and Holleran, 2008).

Abbreviations: acylCer, acylceramide; Cer, ceramide; *CGI-58*, Comparative Gene Identification-58; CLE, bound lipid envelope; DCS, Dorfman–Chanarin syndrome; FA, fatty acid; KC, keratinocyte; NLSDI, neutral lipid storage disorder with ichthyosis; ω -OH, omega hydroxy; SC, stratum corneum; TG, triacylglyceride

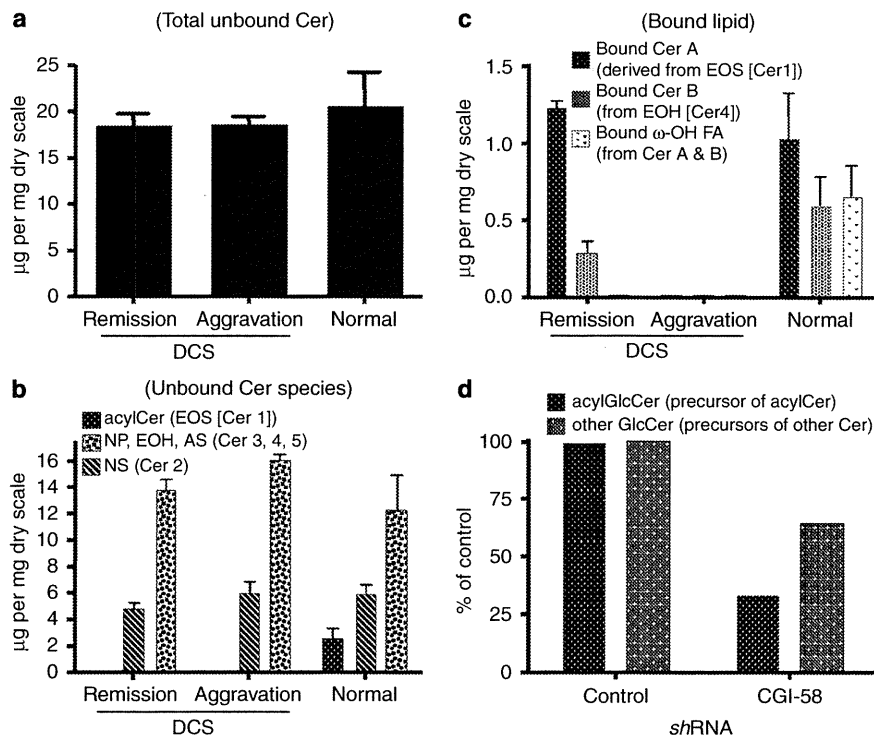


Figure 1. Lipid profile in the stratum corneum. Both unbound acylCer and bound ω -OH Cer deficiencies occur in a Dorfman–Chanarin syndrome (DCS) stratum corneum (SC) (a–c), whereas diminished CGI-58 expression decreases acylglucosylCer production (d). Normal SC from sunburn lesion as controls. CHK transfected with lentivirus-expressed shRNA (CGI-58 or control vector) were cultured in differentiation-inducing medium (Uchida *et al.*, 2001). Lipids were isolated from SC or cells and quantitated using thin-layer chromatography-scanning densitometry as described previously (Uchida *et al.*, 2001). $n = 1$ (DC) and $n = 3$ (normal). All studies were approved by the institutional ethics review boards (Kochi University and University of California, San Francisco) and were performed according to the Declaration of Helsinki Principles.

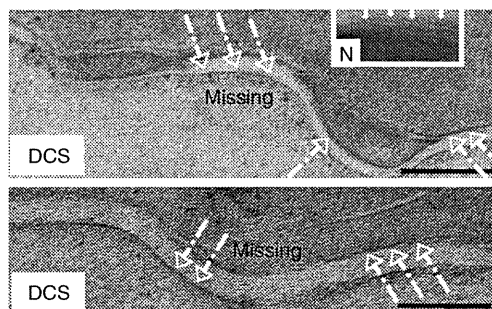


Figure 2. Electron micrographs display lack of continuous lipid monolayer, CLE, in the SC from two DCS patients (Demerjian *et al.*, 2006) vs. normal subject (inset, N). Skin samples were fixed in Karnovsky’s fixative, and post-fixed with ruthenium tetroxide or osmium tetroxide, as previously described (Behne *et al.*, 2000). Ultrathin sections were examined, after further contrasted with lead citrate, with a Zeiss 10A (Carl Zeiss, Thornwood, NY) (Behne *et al.*, 2000). Arrows (with solid line, presence and with dotted line, absence) indicate CLE structures. Bars = 100 nm.

Not only bound ω -OH Cer, but also bound ω -OH FA (resulting from the subsequent hydrolysis of some bound ω -OH Cer by ceramidase) decline significantly in DCS (Figure 1c). As with TG accumulation (Ujihara *et al.*, 2010), the decrease in these bound lipids reflects disease severity. Accordingly,

this patient, as well as in two additional DCS patients (Demerjian *et al.*, 2006), lacked CLE on ultrastructural analysis of affected SC (Figure 2).

Finally, we investigated whether the decreased acylCer in DCS is due to a gain-of-function of mutation in *CGI-58*, rather than a deficiency of

TG-derived FA. A substantial decrease in acylglucosylCer (= acylCer precursor), but not in other glucosylCer species, was evident in lentivirus-expressed CGI-58 shRNA-treated cultured human keratinocytes (Figure 1d). Hence, by facilitating the lipolysis of TG, CGI-58 provides FA for ω -O-esterification leading to acylCer formation. The recent demonstration of a lethal, postnatal permeability barrier defect and deficiency of both acylCer and bound ω -OH Cer in *cgi-58*-null mice (Radner *et al.*, 2009) further supports this conclusion.

We conclude from these and previous studies that CGI-58 not only facilitates TG lipolysis but also provides FA for the ω -O-esterification of Cer leading to acylCer production, as well as bound ω -OH Cer generation leading to CLE formation (see Supplementary Figure S1 online). These studies highlight that the deficiency of an essential barrier constituent, acylCer, likely contributes to the permeability barrier

abnormality in DCS. Although the function of the CLE is still unclear, a role as a necessary scaffold for the lamellar bilayer organization is likely (Uchida and Holleran, 2008). Thus, CLE deficiency, coupled with disorganization of extracellular lamellar bilayers, likely merge to provoke the barrier abnormality in NLSDI (see Supplementary Figure S2 online). Finally, to overcome this metabolic disadvantage in forming the epidermal permeability barrier, epidermal proliferation likely increases, which in turn results in hyperkeratosis, phenotypic features common to virtually all of the ichthyoses (Demerjian *et al.*, 2006; Akiyama *et al.*, 2008), that is, 'A compromised permeability barrier 'drives' the hyperproliferative epidermis in NLSDI and other ichthyoses' (Elias *et al.*, 2008).

CONFLICT OF INTEREST

The authors state no conflict of interest.

ACKNOWLEDGMENTS

We acknowledge Ms Sally Pennypacker for technical support with the cell cultures. This study was supported by an REAC award from the University of California, San Francisco, and National Institutes of Health grant AR051077 (to YU).

Yoshikazu Uchida^{1,2}, Yunhi Cho^{1,2,3}, Sam Moradian^{1,2}, Jungmin Kim^{1,2,3}, Kimiko Nakajima⁴, Debra Crumrine^{1,2}, Kyungho Park^{1,2}, Mayumi Ujihara⁴, Masashi Akiyama⁵, Hiroshi Shimizu⁵, Walter M. Holleran^{1,2,6}, Shigetoshi Sano⁴ and Peter M. Elias^{1,2}

¹Department of Dermatology, School of Medicine, University of California, San Francisco,

San Francisco, California, USA; ²Department of Veterans Affairs Medical Center and Northern California Institute for Research and Education, San Francisco, California, USA; ³Department of Medical Nutrition, Graduate School of East-West Medical Science, Kyung Hee University, Seoul, South Korea; ⁴Department of Dermatology, Kochi Medical School, Kochi University, Nankoku, Japan; ⁵Department of Dermatology, Hokkaido University Graduate School of Medicine, Sapporo, Japan and ⁶Department of Pharmaceutical Chemistry, School of Pharmacy, University of California, San Francisco, San Francisco, California, USA
E-mail: uchiday@derm.ucsf.edu

SUPPLEMENTARY MATERIAL

Supplementary material is linked to the online version of the paper at <http://www.nature.com/jid>

REFERENCES

- Akiyama M, Sakai K, Takayama C *et al.* (2008) CGI-58 is an alpha/beta-hydrolase within lipid transporting lamellar granules of differentiated keratinocytes. *Am J Pathol* 173:1349–60
- Behne M, Uchida Y, Seki T *et al.* (2000) Omega-hydroxyceramides are required for corneocyte lipid envelope (CLE) formation and normal epidermal permeability barrier function. *J Invest Dermatol* 114:185–92
- Bouwstra JA, Gooris GS, Dubbelaar FE *et al.* (1998) Role of ceramide 1 in the molecular organization of the stratum corneum lipids. *J Lipid Res* 39:186–96
- Demerjian M, Crumrine DA, Milstone LM *et al.* (2006) Barrier dysfunction and pathogenesis of neutral lipid storage disease with ichthyosis (Chanarin–Dorfman syndrome). *J Invest Dermatol* 126:2032–8
- Elias PM, Williams ML (1985) Neutral lipid storage disease with ichthyosis. Defective lamellar body contents and intracellular dispersion. *Arch Dermatol* 121:1000–8

- Elias PM, Williams ML, Holleran WM *et al.* (2008) Pathogenesis of permeability barrier abnormalities in the ichthyoses: inherited disorders of lipid metabolism. *J Lipid Res* 49:697–714
- Radner FP, Streith IE, Schoiswohl G *et al.* (2009) Growth retardation, impaired triacylglycerol catabolism, hepatic steatosis, and lethal skin barrier defect in mice lacking comparative gene identification-58 (CGI-58). *J Biol Chem* 285:7300–11
- Schweiger M, Lass A, Zimmermann R *et al.* (2009) Neutral lipid storage disease: genetic disorders caused by mutations in adipose triglyceride lipase/PNPLA2 or CGI-58/ABHD5. *Am J Physiol Endocrinol Metab* 297:E289–96
- Stone SJ, Myers HM, Watkins SM *et al.* (2004) Lipopenia and skin barrier abnormalities in DGAT2-deficient mice. *J Biol Chem* 279:11767–76
- Uchida Y, Behne M, Quiec D *et al.* (2001) Vitamin C stimulates sphingolipid production and markers of barrier formation in submerged human keratinocyte cultures. *J Invest Dermatol* 117:1307–13
- Uchida Y, Holleran WM (2008) Omega-O-acylceramide, a lipid essential for mammalian survival. *J Dermatol Sci* 51:77–87
- Ujihara M, Nakajima K, Yamamoto M *et al.* (2010) Epidermal triglyceride levels are correlated with severity of ichthyosis in Dorfman–Chanarin syndrome. *J Dermatol Sci* 57:102–7
- Vasireddy V, Uchida Y, Salem Jr N *et al.* (2007) Loss of functional ELOVL4 depletes very long-chain fatty acids (>=C28) and the unique (omega)-O-acylceramides in skin leading to neonatal death. *Hum Mol Genet* 16:471–82
- Wertz PW, Downing DT (1990) Metabolism of linoleic acid in porcine epidermis. *J Lipid Res* 31:1839–44
- Yamaguchi T, Osumi T (2009) Chanarin–Dorfman syndrome: deficiency in CGI-58, a lipid droplet-bound coactivator of lipase. *Biochim Biophys Acta* 1791:519–23

Detection of Human Papillomavirus DNA in Plucked Eyebrow Hair from HIV-Infected Patients

Journal of Investigative Dermatology (2010) 130, 2499–2502; doi:10.1038/jid.2010.147; published online 3 June 2010

TO THE EDITOR

The risk of developing human papillomavirus (HPV)-related benign and malignant cutaneous lesions is markedly increased in immunosuppressed people such as organ-transplant recipi-

ents (Harwood *et al.*, 2000) and HIV-infected patients (Grulich *et al.*, 2007; Stier and Baranoski, 2008). Although HPV DNA in plucked eyebrow hair has been well investigated (Boxman *et al.*, 1997) in renal transplant recipients and

immunocompetent patients (ICPs) and correlated with both benign and malignant cutaneous lesions (Struijk *et al.*, 2003; Plasmeijer *et al.*, 2009), very little is known about HPV prevalence in eyebrow hair from HIV patients.

The study design was approved by the research ethics committee and all

Abbreviations: HPV, human papillomavirus; ICP, immunocompetent patient

Department of Health (AF0301). We thank Dr Michele Weiss for the figure illustration.

**Fred M. Kaplan¹,
Michael J. Mastrangelo^{2,3} and
Andrew E. Aplin^{1,3}**

¹Department of Cancer Biology, Thomas Jefferson University, Philadelphia, Pennsylvania, USA; ²Department of Medical Oncology, Thomas Jefferson University, Philadelphia, Pennsylvania, USA and ³Kimmel Cancer Center, Thomas Jefferson University, Philadelphia, Pennsylvania, USA
E-mail: Fred.Kaplan@mail.jc.tju.edu or Andrew.Aplin@KimmelCancerCenter.Org

REFERENCES

- Davies H, Bignell GR, Cox C *et al.* (2002) Mutations of the BRAF gene in human cancer. *Nature* 417:949–54
- Flaherty K, Puzanov I, Sosman J *et al.* (2009) Phase I study of PLX4032: proof of concept for V600E BRAF mutation as a therapeutic target in human cancer. *J Clin Oncol* 27: 15S (Abstract)
- Halaban R, Zhang W, Bacchiocchi A *et al.* (2010) PLX4032, a selective BRAF V600E kinase inhibitor, activates the ERK pathway and enhances cell migration and proliferation of BRAF WT melanoma cells. *Pigment Cell Melanoma Res* 23: 190–200
- Hall-Jackson CA, Eyers PA, Cohen P *et al.* (1999) Paradoxical activation of Raf by a novel Raf inhibitor. *Chem Biol* 6:559–68
- Hatzivassiliou G, Song K, Yen I *et al.* (2010) RAF inhibitors prime wild-type RAF to activate the MAPK pathway and enhance growth. *Nature* 464:431–5
- Heidorn SJ, Milagre C, Whittaker S *et al.* (2010) Kinase-dead BRAF and oncogenic RAS cooperate to drive tumor progression through CRAF. *Cell* 140:209–21
- King AJ, Patrick DR, Batorsky RS *et al.* (2006) Demonstration of a genetic therapeutic index for tumors expressing oncogenic BRAF by the kinase inhibitor SB-590885. *Cancer Res* 66:11100–5
- Michaloglou C, Vredeveld LC, Mooi WJ *et al.* (2008) BRAF(E600) in benign and malignant human tumours. *Oncogene* 27:877–95
- Poulikakos PI, Zhang C, Bollag G *et al.* (2010) RAF inhibitors transactivate RAF dimers and ERK signalling in cells with wild-type BRAF. *Nature* 464:427–30
- Ritt DA, Monson DM, Specht SI *et al.* (2010) Impact of feedback phosphorylation and Raf heterodimerization on normal and mutant B-Raf signaling. *Mol Cell Biol* 30:806–19
- Rushworth LK, Hindley AD, O'Neill E *et al.* (2006) Regulation and role of Raf-1/B-Raf heterodimerization. *Mol Cell Biol* 26:2262–72
- Tsai J, Lee JT, Wang W *et al.* (2008) Discovery of a selective inhibitor of oncogenic B-Raf kinase with potent antimelanoma activity. *Proc Natl Acad Sci USA* 105:3041–6

Complete Paternal Isodisomy of Chromosome 17 in Junctional Epidermolysis Bullosa with Pyloric Atresia

Journal of Investigative Dermatology (2010) **130**, 2671–2674; doi:10.1038/jid.2010.182; published online 1 July 2010

TO THE EDITOR

Uniparental disomy (UPD) is a condition in which two chromosomes of the same pair are inherited in whole or in part from only one parent. There are two types of UPD: uniparental isodisomy and uniparental heterodisomy. The former refers to two identical copies of a single homolog of a chromosome from one parent, and the latter indicates two different chromosome homologs from one parent. UPD can lead to an abnormal phenotype when isodisomy for a chromosome carrying a mutation for an autosomal-recessive disease gene results in homozygosity for the mutation.

Epidermolysis bullosa (EB) is a collection of heterogeneous disorders, in which congenital skin fragility leads to separation of the dermo-epidermal junction. EB has been subdivided into three major groups and one minor group, based on the level of blister formation:

EB simplex, junctional EB, (JEB), dystrophic EB, and Kindler syndrome (Fine *et al.*, 2008). Mutations in 14 different genes have been identified as underlying EB subtypes (Fine *et al.*, 2008; Groves *et al.*, 2010). Among them, mutations in the gene encoding $\alpha 6$ integrin subunit (*ITGA6*) or $\beta 4$ integrin subunit (*ITGB4*) are responsible for one rare subtype of JEB: JEB associated with pyloric atresia (JEB-PA). JEB-PA is inherited autosomal recessively and is characterized by generalized blistering and occlusion of the pylorus at birth, which usually leads to early demise. Most patients with JEB-PA have mutations in *ITGB4*, and more than 60 *ITGB4* mutations have been identified in JEB-PA cases.

The proband was the first child of nonconsanguineous healthy parents. There was no family history of bullous diseases. The child was born by cesarean section after a 35-week gestation

because of polyhydramnion and had a birth weight of 1916 g and a birth length of 46.5 cm. Clinical manifestations of the proband included extensive blistering, especially on the extremities (Figure 1a). Routine abdominal X-ray demonstrated pyloric atresia (PA) (Figure 1b). No abnormalities other than skin fragility and PA were apparent. The proband died of sepsis 2 months after birth.

Immunofluorescence analysis revealed an absence of the $\beta 4$ integrin subunit in skin specimens from the proband (Figure 1c–f). Expression of $\alpha 6$ integrin subunit and plectin was reduced in proband skin samples (Figure 1g and h). Immunostaining for BP230, laminin 332, and type VII collagen revealed normal linear-labeling patterns (Figure 1i–k).

Mutational analysis of all coding exons (exons 2–41) including the exon–intron boundaries of the *ITGB4* revealed that the proband was homozygous for c.953_955del in exon 8 (Figure 2a). The genomic DNA nucleotides, the

Abbreviations: EB, epidermolysis bullosa; JEB, junctional EB; JEB-PA, JEB with pyloric atresia; *ITGA6*, $\alpha 6$ integrin subunit; *ITGB4*, $\beta 4$ integrin subunit; UPD, uniparental disomy

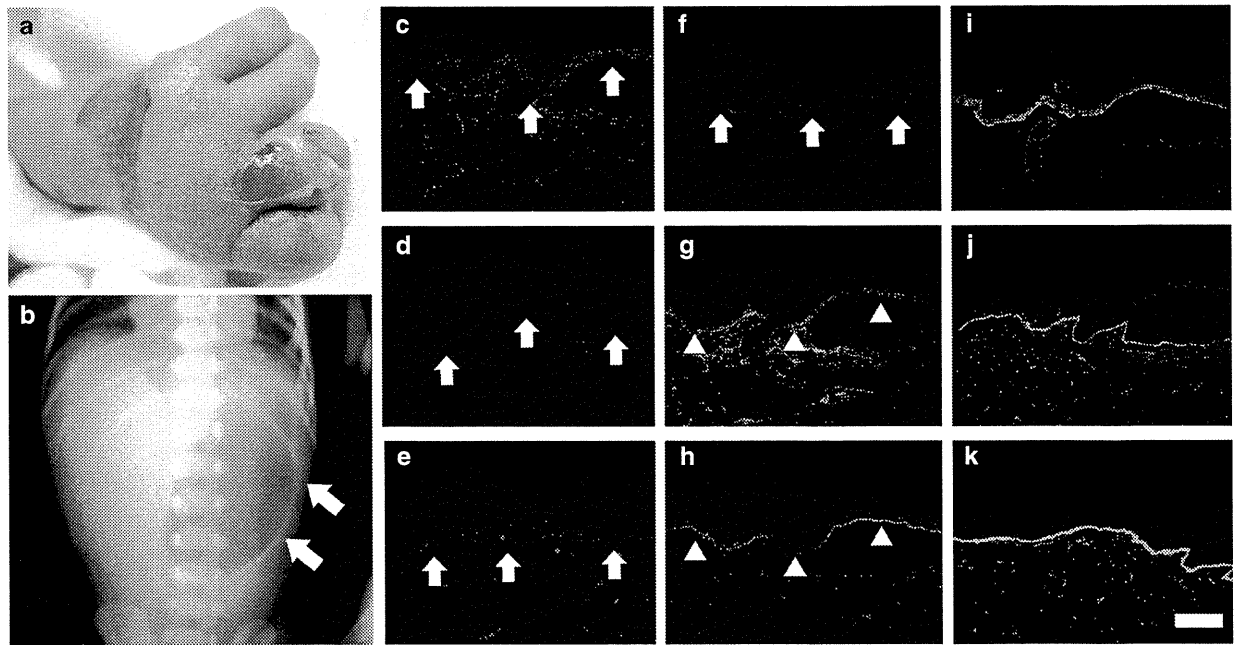


Figure 1. Clinical features of the proband and immunofluorescence analysis. (a) Extensive blistering is seen on the extremities at birth. (b) Abdominal X-ray reveals a single-bubble sign (arrows). β 4 integrin subunit (3E1 (c), 113C (d), 450-9D (e), and 450-11A (f)) is not detected in the proband's skin (arrows). The expression of α 6 integrin subunit (GoH3, g) and plectin (HD1-121, h) is diminished (arrowheads). BP230 (S1193, i), laminin-332 (GB3, j), and type VII collagen (LH7.2, k) show a normal linear staining pattern (scale bar = 100 μ m). HD1-121 was donated by Professor Owaribe of Nagoya University, 113C by Professor Sonnenberg of the Netherlands Cancer Institute, 450-9D and 450-11A by Professor Lankford of the Oak Ridge National Laboratory, and S1193 by Professor Stanley of the University of Pennsylvania.

complementary DNA nucleotides and the amino acids of the protein were numbered based on the following sequence information (GenBank accession no. NM_000213). Mutation c.953_955del is predicted to result in the loss of asparagine at amino acid position 318 (p.Asn318del, Figure 2b), and this deletion mutation is not expected to cause subsequent frame-shift followed by a premature termination codon. Mutation c.953_955del was previously described in two JEB-PA cases (Iacovacci *et al.*, 2003; Varki *et al.*, 2006). The proband's father was heterozygous for this mutation (Figure 2a), although her mother revealed only normal sequences (Figure 2a).

To elucidate the origin of c.953_955del homozygosity in the proband, haplotype analysis of the entire chromosome 17 using 15 microsatellite markers (the ABI Prism Linkage Mapping Set Version 2.5 (Applied Biosystems, Warrington, UK)) was performed. The proband was found to be homozygous for all 15 microsatellite markers (Figure 2d). Ten of the 15 markers were

fully informative for inheritance of two copies of a single paternal chromosome 17 in the proband (Figure 2d). For the non-chromosome 17 markers (D1S468, D1S252, D1S2842, D3S1297, D3S1566 and D3S1311), there were no discrepancies in the segregation of maternal and paternal alleles to the proband, confirming that the mother is indeed the biological mother of the patient (data not shown). Normal karyotyping ruled out monosomy of chromosome 17. The results in this family are compatible with the inheritance of two identical copies of a single chromosome 17 from the proband's father, which indicates complete paternal isodisomy of chromosome 17 in the proband. The medical ethical committee of Hokkaido University approved all the described studies. The study was conducted according to the Declaration of Helsinki Principles. Participants gave their written informed consent.

A recent review of the literature on UPD summarized 197 maternal and 68 paternal cases of UPD (Kotzot and Utermann, 2005). For UPDs of chromosome 17, only a few cases of maternal

heterodisomy have been described (Genuardi *et al.*, 1999; Rio *et al.*, 2001). Recently, UPD of the whole chromosome 17 was reported as maternal heterodisomy of 17q and proximal 17p, and isodisomy of distal 17p (Lebre *et al.*, 2009). As far as we know, uniparental isodisomy of the whole chromosome 17 has not been described in the literature.

More than 35 cases of recessive-inherited disease have been reported as being caused by UPD (Kotzot and Utermann, 2005). UPD has been reported to be responsible for several EB subtypes, including Herlitz JEB (Castori *et al.*, 2008; Fassihi *et al.*, 2005; Pulkkinen *et al.*, 1997; Takizawa *et al.*, 2000; Takizawa *et al.*, 1998), EB simplex with pyloric atresia (Nakamura *et al.*, 2005) and recessive dystrophic EB (Fassihi *et al.*, 2006). So far, JEB-PA has not been described to result from UPD.

p.Asn318del (c.953_955del) has been identified as responsible for JEB-PA in two reports (Iacovacci *et al.*, 2003; Varki *et al.*, 2006). Asn³¹⁸ in β 4 integrin subunit resides in the extracellular

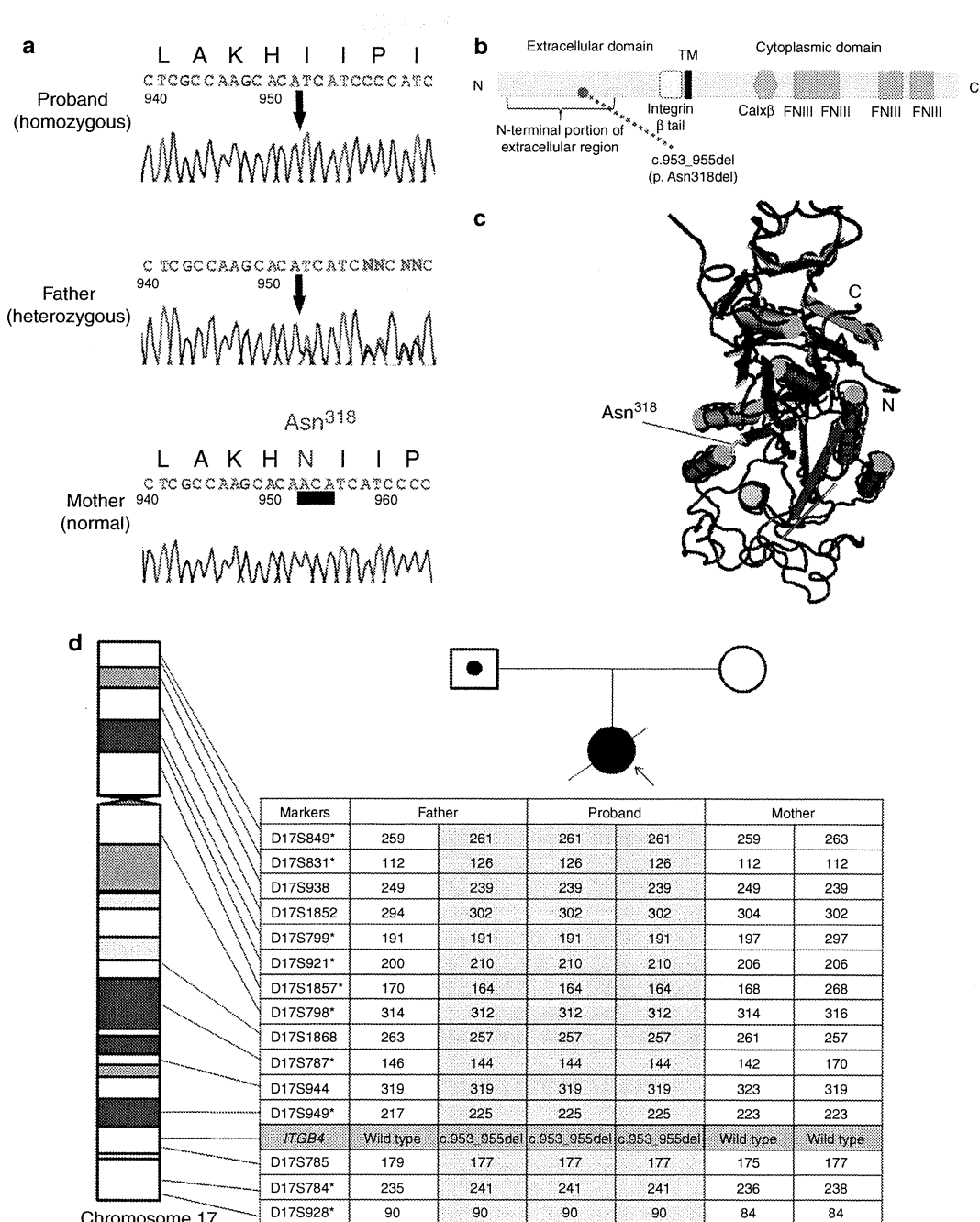


Figure 2. *ITGB4* mutation analysis. (a) The proband is homozygous for c.953_955 del (arrow). The proband's father is heterozygous for c.953_955 del (arrow). In contrast, the mother's gDNA shows only wild-type sequences. Deleted nucleotides are underlined. (b) Schematic arrangement of β4 integrin subunit and the positions of the mutation in the proband. (c) 3D imaging of the N-terminal extracellular domain of the integrin β chain (NCBI Conserved Domain Database (code: smart00187)) was done using Cn3D-4.1 software. Asn³¹⁸ is in the linking loop between the α helix and the β sheet (arrow). (d) The proband was homozygous for all 15 microsatellite markers spanning all of chromosome 17. Ten of the 15 markers (*) suggest that the proband's alleles originated from one homolog of paternal chromosome 17.

domain of the protein (Figure 2b). This asparagine residue is an amino acid that is conserved not only in the β4 integrin subunit of vertebrates but in all the human integrin-β chains (Iacovacci *et al.*, 2003).

The 3D structure of the N-terminal portion of the extracellular domain indicates that Asn³¹⁸ consists of a linking loop between the α helix and the β sheet (Figure 2c). It is possible that the loss of

this asparagine in the extracellular domain leads to significant conformational change and protein instability.

In summary, to our knowledge, we have reported the first case of complete

isodisomy of chromosome 17 and the first example of UPD underlying JEB-PA.

CONFLICT OF INTEREST

The authors state no conflict of interest.

ACKNOWLEDGMENTS

We thank Professor Jouni Uitto for his critical comments on the present case, Ms Yuko Hayakawa and Ms Yuki Miyamura for their technical assistance, and Mr Michael O'Connell for his proofreading. This work was supported in part by grants-in-aid from the Ministry of Education, Culture, Sports, Science and Technology to H. Shimizu (Kiban A 21249063).

Ken Natsuga¹, Wataru Nishie¹, Ken Arita¹, Satoru Shinkuma¹, Hideki Nakamura¹, Shogo Kubota², Sumihisa Imakado³, Masashi Akiyama¹ and Hiroshi Shimizu¹

¹Department of Dermatology, Hokkaido University Graduate School of Medicine, Sapporo, Japan; ²Department of Pediatrics, Japanese Red Cross Medical Center, Tokyo, Japan and ³Department of Dermatology, Japanese Red Cross Medical Center, Tokyo, Japan
E-mail: natsuga@med.hokudai.ac.jp

REFERENCES

- Castori M, Floriddia G, Pisaneschi E *et al.* (2008) Complete maternal isodisomy causing reduction to homozygosity for a novel LAMB3 mutation in Herlitz junctional epidermolysis bullosa. *J Dermatol Sci* 51:58–61
- Fassih H, Lu L, Wessagowit V *et al.* (2006) Complete maternal isodisomy of chromosome 3 in a child with recessive dystrophic epidermolysis bullosa but no other phenotypic abnormalities. *J Invest Dermatol* 126:2039–43
- Fassih H, Wessagowit V, Ashton GH *et al.* (2005) Complete paternal uniparental isodisomy of chromosome 1 resulting in Herlitz junctional epidermolysis bullosa. *Clin Exp Dermatol* 30:71–4
- Fine JD, Eady RA, Bauer EA *et al.* (2008) The classification of inherited epidermolysis bullosa (EB): Report of the Third International Consensus Meeting on Diagnosis and Classification of EB. *J Am Acad Dermatol* 58:931–50
- Genuardi M, Tozzi C, Pomponi MG *et al.* (1999) Mosaic trisomy 17 in amniocytes: phenotypic outcome, tissue distribution, and uniparental disomy studies. *Eur J Hum Genet* 7:421–6
- Groves RW, Liu L, Dopping-Hepenstal PJ *et al.* (2010) A homozygous nonsense mutation within the dystonin gene coding for the coiled-coil domain of the epithelial isoform of BPAG1 underlies a new subtype of autosomal recessive epidermolysis bullosa simplex. *J Invest Dermatol* 130:1551–7
- Iacovacci S, Ciczuzza S, Odoriso T *et al.* (2003) Novel and recurrent mutations in the integrin beta 4 subunit gene causing lethal junctional epidermolysis bullosa with pyloric atresia. *Exp Dermatol* 12:716–20
- Kotzot D, Utermann G (2005) Uniparental disomy (UPD) other than 15: phenotypes and bibliography updated. *Am J Med Genet A* 136:287–305
- Lebre AS, Moriniere V, Dunand O *et al.* (2009) Maternal uniparental heterodisomy of chromosome 17 in a patient with nephropathic cystinosis. *Eur J Hum Genet* 17:1019–23
- Nakamura H, Sawamura D, Goto M *et al.* (2005) Epidermolysis bullosa simplex associated with pyloric atresia is a novel clinical subtype caused by mutations in the plectin gene (PLEC1). *J Mol Diagn* 7:28–35
- Pulkkinen L, Bullrich F, Czarnecki P *et al.* (1997) Maternal uniparental disomy of chromosome 1 with reduction to homozygosity of the LAMB3 locus in a patient with Herlitz junctional epidermolysis bullosa. *Am J Hum Genet* 61:611–9
- Rio M, Ozilou C, Cormier-Daire V *et al.* (2001) Partial maternal heterodisomy of chromosome 17q25 in a case of severe mental retardation. *Hum Genet* 108:511–5
- Takizawa Y, Pulkkinen L, Chao SC *et al.* (2000) Mutation report: complete paternal uniparental isodisomy of chromosome 1: a novel mechanism for Herlitz junctional epidermolysis bullosa. *J Invest Dermatol* 115:307–11
- Takizawa Y, Pulkkinen L, Shimizu H *et al.* (1998) Maternal uniparental meroisodisomy in the LAMB3 region of chromosome 1 results in lethal junctional epidermolysis bullosa. *J Invest Dermatol* 110:828–31
- Varki R, Sadowski S, Pfendner E *et al.* (2006) Epidermolysis bullosa. I. Molecular genetics of the junctional and hemidesmosomal variants. *J Med Genet* 43:641–52

CD44-Deficient Mice Do Not Exhibit Impairment of Epidermal Langerhans Cell Migration to Lymph Nodes after Epicutaneous Sensitization with Protein

Journal of Investigative Dermatology (2010) **130**, 2674–2677; doi:10.1038/jid.2010.170; published online 24 June 2010

TO THE EDITOR

CD44 is a type I transmembrane protein that binds extracellular matrix nonsulfated glycosaminoglycan hyaluronan and has an important role in cell adhesion and migration (Isacke, 2002). Thus, CD44 is involved with leukocyte egress, tumor invasiveness, and metastasis (Isacke, 2002).

The role of CD44 in epidermal Langerhans cell (LC) migration to drain-

ing lymph nodes (LNs) was first evaluated by an antibody blocking system. Antibodies against CD44 epitopes inhibited emigration of LCs from the epidermis and prevented cultured LC binding to T-cell zones in LN-frozen sections (Weiss *et al.*, 1997). In a CD44-deficient mouse system, CD44 deficiency did not impair LC emigration from the epidermis, but significantly influenced their LN homing (Mummert

et al., 2004). In recent years, there has been significant progress in understanding the characteristics and kinetics of LCs. It is known that there are two kinds of Langerin⁺ dendritic cells (DCs) (definition of LCs): one resides in the epidermis and another resides in the dermis (Bursch *et al.*, 2007). They show different migration patterns to draining LNs after immunization. Dermal Langerin⁺ DC migration peaks early at 24 hours, whereas peak migration of epidermal LC is delayed until

Abbreviations: DC, dendritic cell; LC, Langerhans cell; LN, lymph node; Th, T helper

Japanese-Specific Filaggrin Gene Mutations in Japanese Patients Suffering from Atopic Eczema and Asthma

Journal of Investigative Dermatology (2010) 130, 2834–2836; doi:10.1038/jid.2010.218; published online 5 August 2010

TO THE EDITOR

Mutations in *FLG*, the gene encoding profilaggrin/filaggrin, are the underlying cause of ichthyosis vulgaris (OMIM 146700) and an important predisposing factor for atopic eczema (AE) (Sandilands *et al.*, 2007). *FLG* mutations are also significantly associated with asthma with AE mainly in the European population (Rodríguez *et al.*, 2009; van den Oord and Sheikh, 2010). The presence of population-specific *FLG* mutations has been reported in both the European and Asian races (Nomura *et al.*, 2007; Sandilands *et al.*, 2007). To clarify whether *FLG* mutations are a predisposing factor for asthma in the non-European population, we initially studied 172 Japanese AE patients (mean age, 24.8 ± 9.1 years) and 134 unrelated Japanese control individuals (healthy volunteers; mean age, 27.9 ± 6.0 years). All AE patients had been diagnosed based on widely recognized diagnostic criteria (Hanifin and Rajka, 1980). The majority of AE patients and control individuals were identical to those in a previous study (Nemoto-Hasebe *et al.*, 2010). In this AE cohort, 73 AE patients (mean age, 25.4 ± 8.9 years) experienced complications with asthma. Furthermore, we studied another Japanese asthma cohort (137 patients; mean age, 58.2 ± 16.9 years). Patients were considered asthmatic based on the presence of recurrent episodes of ≥ 2 of the three symptoms (coughing, wheezing, or dyspnea) associated with demonstrable reversible airflow limitation, either spontaneously or with an inhaled short-acting β_2 -agonist and/or increased airway responsiveness to methacholine (Isada *et al.*, 2010). Fully informed consent was obtained from the participants or their legal guardians for this

study. This study had been approved by the Ethical Committee at Hokkaido University Graduate School of Medicine and was conducted according to the Declaration of Helsinki Principles.

FLG mutation screening revealed that 27.4% of patients in our Japanese AE complicated with asthma case series carried one or more of the eight *FLG* mutations (combined minor allele frequency of 0.151, $n=146$) (Table 1). Conversely, 26.3% of Japanese AE patients without asthma carried one or more of the eight *FLG* mutations (combined minor allele frequency of 0.147, $n=198$). The *FLG* variants are also carried by 3.7% of Japanese control individuals (combined minor allele frequency of 0.019, $n=268$). We found that all compound heterozygous mutations were present in *trans* by observing transmission or haplotype analysis (Nomura *et al.*, 2007, 2008). There is a statistically significant association between the eight *FLG* mutations and AE with asthma, and between the eight *FLG* mutations and AE without asthma (Table 1). Moreover, AE complicated with asthma manifested in heterozygous carriers of *FLG* mutations with an odds ratio for AE and asthma of 9.74 (95% confidence interval 3.47–27.32), suggesting a relationship between *FLG* mutations and AE with asthma.

In the Japanese general asthma cohort, 8.0% of the asthma patients carried one or more of the eight *FLG* mutations (combined minor allele frequency of 0.04, $n=274$) (Table 2). Whereas, of the Japanese patients with asthma complicated by AE, 22.2% carried one or more of the *FLG* mutations (combined minor allele frequency of 0.11, $n=36$). In contrast, 5.9% of asthma patients without AE carried one or more of the *FLG* mutations

(combined minor allele frequency of 0.03, $n=238$). There was a statistically significant association between the eight *FLG* mutations and asthma with AE (Table 2). There was no statistically significant association between the *FLG* mutations and entire asthma patients, nor between *FLG* mutations and asthma without AE. We cannot exclude the possibility that this lack of significant association is due to the small number of the patients included in this study. We used the same control set for both case-controlled studies. Thus, strictly speaking, there is no independent replication for the control group.

Recent meta-analysis revealed that *FLG* mutations are significantly associated with asthma in the European population and there are especially, strong effects observed for *FLG* mutations for the compound phenotype, asthma in addition to eczema (Rodríguez *et al.*, 2009; van den Oord and Sheikh, 2010). In contrast, there appeared to be no association of *FLG* mutations with asthma in the absence of eczema (Rodríguez *et al.*, 2009; van den Oord and Sheikh, 2010).

This Japanese cohort has a completely different *FLG* mutation spectrum from those in the European and the North American populations. However, our results clearly confirm the strong association of *FLG* mutations with our Japanese cohort of AE patients with asthma complications, and the association of *FLG* mutations and asthma patients with AE complications, for the first time outside Europe or North America. Conversely, this study showed no significant correlation between general asthma patients and *FLG* mutations, suggesting that atopic asthma patients associated with *FLG* mutations are a minority among general asthma patients. The frequency of heterozygous, compound heterozygous, and homozygous *FLG* mutation carriers

Abbreviation: AE, atopic eczema

Table 1. Atopic eczema case-control association analysis for *FLG* null variants in Japan

Genotype	R501X		3321delA		S1695X		Q1701X		S2554X		S2889X		S3296X		K4022X		Combined			
	Con	AE	Con	AE	Con	AE	Con	AE	Con	AE	Con	AE	Con	AE	Con	AE	Con	AE (total)	AE (asthma+)	AE (asthma-)
AA	134	172	133	163	133	172	134	169	133	162	132	152	134	166	134	169	129	126	53	73
Aa	0	0	1	9	1	0	0	3	1	10	2	20	0	6	0	3	5	41	18	23
aa	0	0	0	0	0	0	0	0	0	0	0	0	0	0	0	0	0	5 ¹	2	3
Total	134	172	134	172	134	172	134	172	134	172	134	172	134	172	134	172	134	172	73	99

Abbreviations: AE, atopic eczema; CI, confidence interval; Con, healthy control; OR, odds ratio.
For combined genotype: AE+asthma, exact *P*-value of Pearson χ^2 -test=1.909 \times 10⁻⁶, OR and 95% CI for dominant models (AA vs aX)=9.737 (3.473–27.322); AE–asthma, exact *P*-value of Pearson χ^2 -test=7.189 \times 10⁻⁷, OR and 95% CI for dominant models (AA vs aX)=9.191 (3.383–24.938); all AE, exact *P*-value of Pearson χ^2 -test=1.189 \times 10⁻⁷, OR and 95% CI for dominant models (AA vs aX)=9.416 (3.625–24.450).
¹All the five patients were compound heterozygotes for minor alleles.

Table 2. Asthma case-control association analysis for *FLG* null variants in Japan

Genotype	R501X		3321delA		S1695X		Q1701X		S2554X		S2889X		S3296X		K4022X		Combined			
	Con	Asthma	Con	Asthma	Con	Asthma	Con	Asthma	Con	Asthma	Con	Asthma	Con	Asthma	Con	Asthma	Con	Asthma (total)	Asthma (AE+)	Asthma (AE-)
AA	134	137	133	137	133	137	134	137	133	133	132	132	134	136	134	136	129	126	14	112
Aa	0	0	1	0	1	0	0	0	1	4	2	5	0	1	0	1	5	11	4	7
aa	0	0	0	0	0	0	0	0	0	0	0	0	0	0	0	0	0	0	0	0
Total	134	137	134	137	134	137	134	137	134	137	134	137	134	137	134	137	134	137	18	119

Abbreviations: AE, atopic eczema; CI, confidence interval; Con, healthy control; OR, odds ratio.
For combined genotype: asthma+AE, exact *P*-value of Pearson χ^2 -test=0.0122, OR and 95% CI for dominant models (AA vs aX)=7.3692 (1.7715–30.6748); asthma–AE, exact *P*-value of Pearson χ^2 -test=0.5563, OR and 95% CI for dominant models (AA vs aX)=1.6124 (0.4979–5.2219); all asthma, exact *P*-value of Pearson χ^2 -test=0.1968, OR and 95% CI for dominant models (AA vs aX)=2.2523 (0.7609–6.6667).

observed in our Japanese controls was only 3.7%, which was much lower than that seen in European general population, where it is approximately 7.5%. This suggested that there may be further mutations yet to be discovered in the Japanese. As we have sequenced more than 40 Japanese families with ichthyosis vulgaris, there is now little possibility that further highly prevalent mutations will be found in the Japanese population. However, it is still possible that there might be multiple, further low-frequency *FLG* mutations discovered in the Japanese population. In addition, because of the relatively small sample size of this genetic study, further replication in association studies will be required for *FLG* mutations and asthma in Japan.

In our cohorts, serum IgE levels were extremely high (median, 3141.9 IU ml⁻¹; 25th–75th percentiles, 1276.0–9753.0 IU ml⁻¹) in AE patients with asthma (*n*=73) in the AE cohort, compared with that in total asthma patients (median,

156.0 IU ml⁻¹; 25th–75th percentiles, 71.05–441.45 IU ml⁻¹, *n*=137) in the asthma cohort. These findings suggest that extrinsic allergic sensitization might have an important role in atopic asthma pathogenesis. Recent studies hypothesized skin barrier defects caused by *FLG* mutation(s) allow allergens to penetrate the skin, resulting in initiation of further immune response and leading to the development of systemic allergies, including atopic asthma (Fallon *et al.*, 2009). In patients with asthma that also harbor *FLG* mutations, we could not exclude the possibility that the systemic effects of early eczema might simply influence airway responsiveness (Henderson *et al.*, 2008).

CONFLICT OF INTEREST

Irwin McLean has filed patents relating to genetic testing and therapy development aimed at the filaggrin gene.

ACKNOWLEDGMENTS

We thank the patients and their families for their participation. We also thank Kaori Sakai for fine technical assistance and Dr James McMillan for proofreading and comments concerning this

paper. This work was supported in part by Grants-in-Aid from the Ministry of Education, Science, Sports, and Culture of Japan to M Akiyama (Kiban B 20390304) and by the Health and Labour Sciences Research Grant (Research on Allergic Diseases and Immunology; H21-Meneki-Ippan-003) to H Shimizu. Filaggrin research in the McLean laboratory was supported by grants from The British Skin Foundation; The National Eczema Society; The Medical Research Council (Reference number G0700314); A*STAR, Singapore, and donations from anonymous families affected by eczema in the Tayside region of Scotland.

Rinko Osawa¹, Satoshi Konno², Masashi Akiyama¹, Ikue Nemoto-Hasebe¹, Toshifumi Nomura^{1,3}, Yukiko Nomura¹, Riichi Abe¹, Aileen Sandilands³, W.H. Irwin McLean³, Nobuyuki Hizawa^{4,5}, Masaharu Nishimura² and Hiroshi Shimizu¹

¹Department of Dermatology, Hokkaido University School of Medicine, Sapporo, Japan; ²First Department of Medicine, Hokkaido University School of Medicine, Sapporo, Japan; ³Epithelial Genetics Group, Division of Molecular Medicine, University of Dundee, Colleges of Life Sciences and Medicine, Dentistry & Nursing, Dundee, UK;

⁴Department of Pulmonary Medicine, Institute of Clinical Medicine, Graduate School of Comprehensive Human Sciences, University of Tsukuba, Tsukuba, Ibaraki, Japan and ⁵University Hospital, University of Tsukuba, Tsukuba, Ibaraki, Japan
E-mail: akiyama@med.hokudai.ac.jp

REFERENCES

- Fallon PG, Sasaki T, Sandilands A et al. (2009) A homozygous frameshift mutation in the mouse *Flg* gene facilitates enhanced percutaneous allergen priming. *Nat Genet* 41: 602–8
- Hanifin JM, Rajka G (1980) Diagnostic features of atopic dermatitis. *Acta Derm Venereol* 92:44–7
- Henderson J, Northstone K, Lee SP et al. (2008) The burden of disease associated with filaggrin mutations: a population-based, longitudinal birth cohort study. *J Allergy Clin Immunol* 121:872–7
- Isada A, Konno S, Hizawa N et al. (2010) A functional polymorphism (-603A → G) in the tissue factor gene promoter is associated with adult-onset asthma. *J Hum Genet* 55: 167–74
- Nemoto-Hasebe I, Akiyama M, Nomura T et al. (2010) *FLG* mutation p.Lys4021X in the C-terminal imperfect filaggrin repeat in Japanese atopic eczema patients. *Br J Dermatol* 161:1387–90
- Nomura T, Akiyama M, Sandilands A et al. (2008) Specific filaggrin mutations cause ichthyosis vulgaris and are significantly associated with atopic dermatitis in Japan. *J Invest Dermatol* 128:1436–41
- Nomura T, Sandilands A, Akiyama M et al. (2007) Unique mutations in the filaggrin gene in Japanese patients with ichthyosis vulgaris and atopic dermatitis. *J Allergy Clin Immunol* 119:434–40
- Rodríguez E, Baurecht H, Herberich E et al. (2009) Meta-analysis of filaggrin polymorphisms in eczema and asthma: robust risk factors in atopic disease. *J Allergy Clin Immunol* 123:1361–70
- Sandilands A, Terron-Kwiatkowski A, Hull PR et al. (2007) Comprehensive analysis of the gene encoding filaggrin uncovers prevalent and rare mutations in ichthyosis vulgaris and atopic eczema. *Nat Genet* 39:650–4
- van den Oord RA, Sheikh A (2010) Filaggrin gene defects and risk of developing allergic sensitisation and allergic disorders: systematic review and meta-analysis. *BMJ* 339:b2433

See related commentary on pg 2703

RNase 7 Protects Healthy Skin from *Staphylococcus aureus* Colonization

Journal of Investigative Dermatology (2010) 130, 2836–2838; doi:10.1038/jid.2010.217; published online 29 July 2010

TO THE EDITOR

The Gram-positive bacterium *Staphylococcus aureus* is an important pathogen that causes various skin infections (Miller and Kaplan, 2009). However, healthy skin is usually not infected by *S. aureus*, despite the high carrier rates in the normal population (Noble, 1998). This suggests that the cutaneous defense system has the capacity to effectively control the growth of *S. aureus*. There is increasing evidence that antimicrobial proteins are important effectors of the cutaneous defense system (Harder et al., 2007). A recent study reported that keratinocytes contribute to cutaneous innate defense against *S. aureus* through the production of human β -defensin-3 (Kisich et al., 2007). In addition to human β -defensin-3, other antimicrobial proteins may also participate in cutaneous defense against *S. aureus*. One candidate is RNase 7, a potent antimicrobial ribonuclease that is highly expressed in healthy skin (Harder and Schröder, 2002; Köten et al., 2009).

To investigate the hypothesis that RNase 7 may contribute to protect

healthy skin from *S. aureus* colonization, we first incubated natural RNase 7 isolated from stratum corneum skin extracts (Harder and Schröder, 2002) with *S. aureus* (ATCC 6538). In concordance with our initial report about RNase 7 (Harder and Schröder, 2002), we verified that RNase 7 exhibited

a high killing activity against *S. aureus* (lethal dose of 90% = 3–6 $\mu\text{g ml}^{-1}$).

Recently, we reported a moderate induction of RNase 7 mRNA expression in primary keratinocytes treated with heat-killed *S. aureus* (Harder and Schröder, 2002). To assess the induction of RNase 7 by *S. aureus* in the

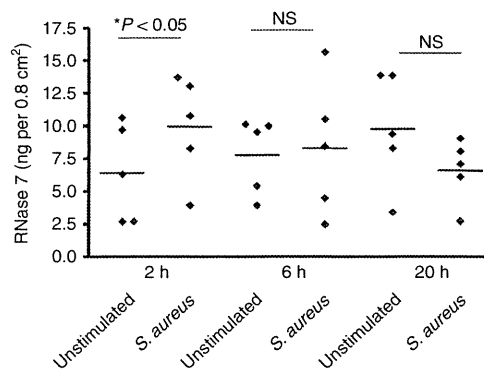


Figure 1. Induced secretion of RNase 7 on the skin surface on treatment with living *S. aureus*.

Defined areas (0.8 cm²) of skin explants derived from plastic surgery were incubated with or without approximately 1,000 colony-forming units of *S. aureus* (ATCC 6538) in 100 μl of sodium phosphate buffer. After 2, 6, and 20 hours, the concentration of secreted RNase 7 was determined by ELISA. Stimulation with *S. aureus* for 2 hours revealed a significant induction as compared with the unstimulated control after 2 hours (*P < 0.05, Student's *t*-test; n.s. = not significant). Data shown are means of triplicates of five skin explants derived from five donors.